

AFRL-IF-RS-TR-2003-9
Final Technical Report
January 2003



ENHANCEMENT OF THE MONET/ATONET WASHINGTON DC NETWORK

Telcordia Technologies

Sponsored by
Defense Advanced Research Projects Agency
DARPA Order No. J792


APPROVED FOR PUBLIC RELEASE; DISTRIBUTION UNLIMITED.


The views and conclusions contained in this document are those of the authors and should not be interpreted as necessarily representing the official policies, either expressed or implied, of the Defense Advanced Research Projects Agency or the U.S. Government.

AIR FORCE RESEARCH LABORATORY
INFORMATION DIRECTORATE
ROME RESEARCH SITE
ROME, NEW YORK

This report has been reviewed by the Air Force Research Laboratory, Information Directorate, Public Affairs Office (IFOIPA) and is releasable to the National Technical Information Service (NTIS). At NTIS it will be releasable to the general public, including foreign nations.

AFRL-IF-RS-TR-2003-9 has been reviewed and is approved for publication

APPROVED: 
ROBERT L. KAMINSKI
Project Engineer

FOR THE DIRECTOR: 
WARREN H. DEBANY, Technical Advisor
Information Grid Division
Information Directorate

REPORT DOCUMENTATION PAGE			<i>Form Approved</i> <i>OMB No. 074-0188</i>	
Public reporting burden for this collection of information is estimated to average 1 hour per response, including the time for reviewing instructions, searching existing data sources, gathering and maintaining the data needed, and completing and reviewing this collection of information. Send comments regarding this burden estimate or any other aspect of this collection of information, including suggestions for reducing this burden to Washington Headquarters Services, Directorate for Information Operations and Reports, 1215 Jefferson Davis Highway, Suite 1204, Arlington, VA 22202-4302, and to the Office of Management and Budget, Paperwork Reduction Project (0704-0188), Washington, DC 20503				
1. AGENCY USE ONLY (Leave blank)	2. REPORT DATE JANUARY 2003	3. REPORT TYPE AND DATES COVERED Final May 00 – Dec 02		
4. TITLE AND SUBTITLE ENHANCEMENT OF THE MONET/ATONET WASHINGTON DC NETWORK		5. FUNDING NUMBERS C - F30602-00-C-0167 PE - 62301E PR - J792 TA - 03 WU - A1		
6. AUTHOR(S) Janet Jackel				
7. PERFORMING ORGANIZATION NAME(S) AND ADDRESS(ES) Telcordia Technologies, Incorporated 445 South Street Morristown NJ 07960-6438		8. PERFORMING ORGANIZATION REPORT NUMBER N/A		
9. SPONSORING / MONITORING AGENCY NAME(S) AND ADDRESS(ES) Defense Advanced Research Projects Agency AFRL/IFG 3701 North Fairfax Drive Arlington Virginia 22203-1714		10. SPONSORING / MONITORING AGENCY REPORT NUMBER AFRL-IF-RS-TR-2003-9		
11. SUPPLEMENTARY NOTES AFRL Project Engineer: Robert L. Kaminski/IFG/(315) 330-1865/ Robert.Kaminski@rl.af.mil				
12a. DISTRIBUTION / AVAILABILITY STATEMENT APPROVED FOR PUBLIC RELEASE; DISTRIBUTION UNLIMITED.			12b. DISTRIBUTION CODE	
13. ABSTRACT (Maximum 200 Words) Report discusses efforts to design, develop, implement, support, and demonstrate experimental activities performed on the MONET/ATDNet network and between MONET/ATDNet and other Next Generation Internet research networks. The report also describes research in the use of hierarchical multiplexing approaches for more efficient use of multi-wavelength networks and enhancements to the MONET Network Control & Management System. Specific experiments were performed for: (1) high speed transmission with alternative modulation formats (such as RZ) with a long term goal of demonstrating 40 Gbit/sec transmission between two nodes in the MONET Network; (2) exploring the limits on transmission of non-SONET rates (major example of which is SMPTE 292M 1.5 Gbit/sec high definition television format) and find ways to extend the transmission to all MONET nodes with improved performance; and (3) exploring network stability, including addition of noise due to multipath interference and polarization effects and network behavior in the presence of transients, such as added and dropped channels.				
14. SUBJECT TERMS Optical Networking, Wavelength Division Multiplexing, Network Control and Management			15. NUMBER OF PAGES 66	
			16. PRICE CODE	
17. SECURITY CLASSIFICATION OF REPORT UNCLASSIFIED	18. SECURITY CLASSIFICATION OF THIS PAGE UNCLASSIFIED	19. SECURITY CLASSIFICATION OF ABSTRACT UNCLASSIFIED	20. LIMITATION OF ABSTRACT UL	

Table of Contents

1	Introduction: Description of the Project	1
1.1	Task 1: Continuation and extension of the MONET Project.....	2
1.1.1	Data Communications Network (DCN) Maintenance.....	2
1.1.2	Network Control and Management (NC&M) System Maintenance	2
1.1.3	Experiments on the MONET/ATDNet Network	3
1.1.4	Experiments on the NGI SuperNet	4
1.2	Task 2: Hierarchical Multiplexing	4
1.3	Summary of accomplishments	4
2	Task 1 Results.....	5
2.1	Network maintenance and NC&M for experiment support.....	5
2.1.1	DCN Maintenance	5
2.1.2	Network Control and Management: Maintenance and Experimental support.....	5
2.2	Network experiments	7
2.2.1	Transmission experiments	9
2.2.2	Network stability.....	10
2.2.3	Network Dynamics	14
2.2.4	NC&M Experiments	26
2.2.5	Other	26
3	Task 2 Results.....	27
3.1	Why Hierarchical Multiplexing?	27
3.2	Hierarchical Wavelength Multiplexing.....	28
3.3	Subcarrier Multiplexing.....	33
3.4	Multiwavelength source for Hierarchical multiplexing: wavebanding and OCDMA	33
3.5	Assessing hierarchical multiplexing	35
3.6	Publications.....	36
4	Lessons learned.....	37
5	Appendix 1: Interactions with other projects.....	38
6	Appendix 2: Publications/Patents	38

Table of Figures

Figure 1 The MONET/ATDNet DC Network at the end of the MONET Project and at the beginning of the MONET Follow-On Project	1
Figure 2 Schematic picture of the relationship between network management and network elements	6
Figure 3 The Lucent Network Element, showing (a) overall architecture, and (b) architecture of the Lithium Niobate switch fabric.	8
Figure 4 Tellium Network element as described in the text	9
Figure 5 Relative noise from several sources. Note that noise from ASE, whether polarized or unpolarized, does not build as a larger number of network elements are traversed. Noise builds rapidly due to multipath interference when the source is highly coherent.	11
Figure 6 Crosstalk and signal in channel 4, offset from each other by about 0.5 nm.....	12
Figure 7 Upper trace shows signal sent from NSA to NASA and back, with crosstalk from signal originating at DARPA separated from monitored signal by 0.2 nm. Crosstalk generating signal is sent twice through the NE in order to maximize effect. Lower trace shows returned signal with same crosstalk, but separated from signal by 0.3 nm. In both cases polarization of incoming signal has been tuned to give maximum impairment.	12
Figure 8 Signal and crosstalk as above, separated by 0.2 nm. Polarization of signal manipulated to produce maximum (upper trace) or minimum (lower trace) effect on eye pattern.....	13
Figure 9 Measured correlation of DGD, wind speed, and wind gusting for a span of fiber.....	14
Figure 10 Switched channel and accompanying channel after NSA-NRL-NSA. Two channels have are shown on different scales; actual CW power in each is approximately equal . Total time is 500 μ s.....	15
Figure 11 Output of CCI-OUT for a CCI-IN to CCI-OUT path (power added and dropped in the same NE without passing into the network) for a modulated input. Because modulation is less than 100%, EDFA gain increases during "off" period.....	17
Figure 12 Modulated channel after passing through network to NRL and back to NSA: two single wavelength EDFAs and six common EDFAs. Impairment is greatest when only two channels are present (lightly loaded) than when the network is fully loaded., and for partial loading, the impairment is intermediate.....	17
Figure 13 Power through the network for the modulated channel and a bystander channel, when only two channels are present. Impairment of the bystander channel is greater when the modulated channel enters the "on" state than when its power is decreased.	18
Figure 14 Bursts passing through the Firstwave NE experience much less distortion than those passing through the Lucent NE, but competition between amplifier dynamics and hardware/software driven gain control in the multichannel EDFA's can lead to unpredictable behavior.....	18
Figure 15 Bursts of varying lengths after passing through the Firstwave Network Element, as shown above.....	19
Figure 16 Burst Mode transmitter/receiver.....	20
Figure 17a Burst sent from NSA-NRL-NSA along with recovered data, and a measure of errors.	21
Figure 17b Same as above, but using burst support.....	21
Figure 18 (left) SOA embedded in laser structure, with lasing only if input power drops below expected signal level. (right) Spectrum of combined signal and burst support wavelengths, compared with width of channel.....	22

Figure 19 Data burst (in center) followed by optically generated burst support. Rise time for burst support power is less than 1 microsecond.....	23
Figure 20 240 μ s burst after CCI-IN to CCI-OUT path, (a) with and (b) without burst support. With burst support the burst is not distorted. In both cases the bursts occupy the same portion of the trace.....	23
Figure 21 Multiple bursts (a) bursts generated by transmitter (b) after passing through the network, with burst support, (c) errors: low level indicates no error and high indicates error. Errors are expected when no signal is present.....	23
Figure 22 Returned data after path from NSA to NASA to NSA, with 13 μ s dropout. (a) With no optical burst support, returned power has large swings. (b) With SOA optical burst support, returned power has no large swings. Arrows indicate period of dropout.....	24
Figure 23 Errors are seen after dropout when there is no optical burst support (a) but not when SOA-OBS is used (b) Scale is 8 μ s/division.....	25
Figure 24 BossNet connection in ATDNet to BOSSNet direction.....	27
Figure 25 Summarizes work on Hierarchical Multiplexing.....	28
Figure 26 Source for 4 2.5 Gb/s channels carried in a single MONET wavelength channel.....	29
Figure 27 (a) Experiment at LTS on the MONET/ATDNet DC Network,, with four 2.5 Gb/s subchannels added at a single wavelength port, passed through the network to NRL, through the network element at NRL, and then dropped through the originating network element at LTS.....	30
Figure 28 BER for the 4 x 2.5 Gb/s experiment at the MONET/ATDNet DC Network.....	30
Figure 29 BER for the four channels.....	31
Figure 30 Comparison of output spectrum for two paths through the West Ring, one through a combination of Lucent and Firstwave NE's and the other through Firstwave NE's only....	33
Figure 31 Summarized results to date.....	33
Figure 32 Modelocked laser multiwavelength source, and transmission experiment for 6.25 and 10 Gb/s. Optical portion of the laser lies within the shaded box.....	34
Figure 33 Recovered data, optical spectrum, and BER, using the mode locked laser of Figure 32 as a source of short pulses.....	35

**Enhancement of the MONET/ATDNet Washington DC Network
DARPA Contract F30602-00-C-0167**

**Final Technical Report
October 31, 2002**

Janet Jackel, Telcordia Technologies

1 Introduction: Description of the Project

This is the final report for Contract F30602-99-C-0167, “Enhancement of the MONET/ATDNet Washington DC Network,” which we will also refer to as the “MONET Follow-On” project. This project followed the 5-year MONET Project, which designed and built the MONET/ATDNet DC network connecting six US Government Agencies in the DC metropolitan area.

The MONET project was a five-year project established to define, demonstrate, and determine how best to achieve multiwavelength optical networking serving both commercial and specialized government applications. The MONET consortium was formed to advance this program, and participants were AT&T, Lucent Technologies, Telcordia Technologies, Bell Atlantic, BellSouth, SBC, and Pacific Telesis, with close working collaborations with the National Security Agency and the Naval Research Laboratory.

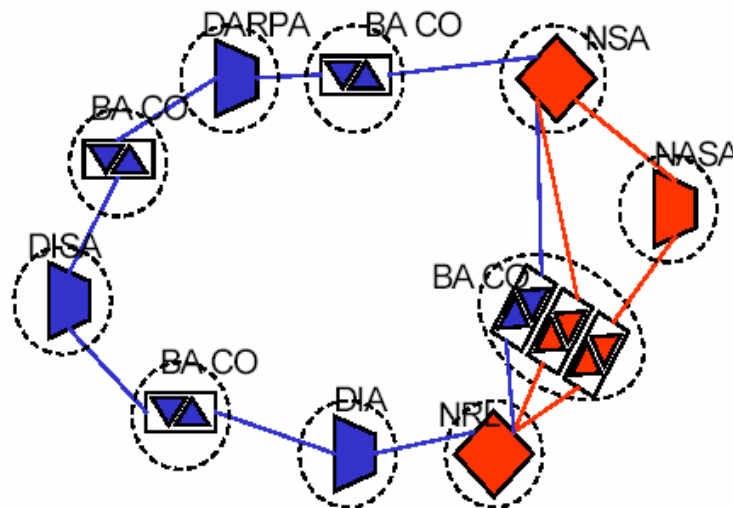


Figure 1 The MONET/ATDNet DC Network at the end of the MONET Project and at the beginning of the MONET Follow-On Project

The MONET project envisioned a transparent, reconfigurable, scalable optical layer encompassing local exchange networks, long distance networks, and even high-end private networks, providing a flexible and broadband infrastructure for building networks at the higher layers, such as SONET, ATM, and IP. This was an ambitious vision when it was first proposed, in 1994, before the first commercial WDM transport systems had been introduced.

As Figure 1 shows, the network at the end of the MONET Project consisted of six add/drop nodes, shown on the figure as either Wavelength Add/Drop Multiplexers (WADMs) or Wavelength Selective Cross-Connects (WSXCs). In this network, the functional difference between a WSXC and a WADM is that WSXCs support four transport (multiwavelength) interfaces while WADMs support only two. Each of the six nodes is capable of adding and dropping a total of eight wavelengths. Between these six add/drop nodes are a number of Wavelength AMPLifiers (WAMPs) which provide optical gain but have no add/drop capability. The network consists of two interconnected rings, an East ring and a West ring.

The details of the network elements and the network have been presented in the reports of the MONET Project. Experiments on this network were begun during the MONET Project, but were limited by the short time between the final installation of the network (summer 1999) and the end of the project in Fall of 1999. Consequently, the MONET Follow-On was begun to maintain the network, to continue the experiments that had been begun, and to look towards more advanced optical networks.

Within the MONET Follow-On Project there were two main tasks. Task 1 provides a base of support for the operation of the network and for experiments on the network, and carries out experiments that are essentially continuations or extensions of those either begun or proposed during the MONET Project. Task 2 breaks new ground, looking at how a transparent and reconfigurable network can evolve to provide greater bandwidth and flexibility by employing some form of “hierarchical multiplexing.”

1.1 Task 1: Continuation and extension of the MONET Project

The Task of extending the original MONET Project requires that certain basic network functions be maintained and to some extent improved. The goal of doing so is to make it possible to continue using the network and to enable experiments, some of which go beyond the original design of the network. A number of categories of work are considered below; the first two are enablers and the last and largest is the set of experiments.

1.1.1 Data Communications Network (DCN) Maintenance

Goal: To maintain DCN connectivity to all Network Elements with a DCN down time not to exceed 1 day/month. Troubleshooting and repair is not to exceed 3 days except for failures in major subsystems (workstations and ATM switches).

1.1.2 Network Control and Management (NC&M) System Maintenance

Goal: The NC&M system that was deployed under the original MONET project was an aggressive effort to push the state of distributed software development. While this was an

important software research goal, the resulting system was not as stable or reliable as it could have been, largely as a result of instabilities in the licensed CORBA environment. During this project we had no charter to redesign the NC&M system but we could make minor modifications to the existing system, collapsing and simplifying its structure and consolidating processes to enhance reliability.

Comments: NC&M is a large topic, suitable for research on its own, but in the context of this project, NC&M is primarily an enabler. This Task was eliminated during the descope of the project in early 2002, in part because of lack of funding and in part because we felt that the primary goals had already been accomplished.

1.1.3 Experiments on the MONET/ATDNet Network

The above two subtasks exist primarily as enablers for the experiments task, which is the centerpiece of the project.

The overall goal of the experiments tasks is to carry out optical layer experiments on the MONET network to determine and document the limits of this technology and, when possible, find ways to extend those limits.

The experiments we have conducted fall into several main categories, with some overlaps:

1. Transmission over the network of **various data rates and formats**, including high speed RZ data and non-SONET rates. The goal is to use the transparency of the network to transmit data that could not be supported by a more conventional network, and to probe the limits of transparency.
2. Experiments exploring **network stability**, including behaviors affected by the addition of noise due to multipath interference and polarization effects, looking for time varying behavior even when the network is in a static state, with neither any changes in connections nor any rapidly varying puts. These experiments were motivated in part by the observation of “error storms” during the MONET Project.
3. Experiments exploring **dynamic network behavior** in the presence of optical transients, such as added and dropped channels or rapidly changing input power. Among the goals of this work were to find ways when possible to overcome the limits of the existing network elements and to identify and document any fundamental technical barriers limiting the use of bursts on transparent optical networks.
4. **Network management** experiments to test the performance of the NC&M system in making rapid connections and rearrangements. These probe not only the limits of the NC&M capabilities, but also make possible many of the experiments testing network dynamic behavior.
5. Continue to perform experiments in **optical layer protection** that are of interest to the MONET/ATDNet community. This goal was eliminated during the descope of the program. Most of the required optical layer protection experiments were in fact completed by the end of the MONET Project.

6. Participate in network trouble-shooting and fault isolation as necessary to keep the experimental network operating. As part of this work, we have shared experimental results with our collaborators, primarily at LTS, NRL, DISA and LPS, through direct interactions and informal meetings.

1.1.4 Experiments on the NGI SuperNet

We have an additional goal of demonstrating interconnections with other NGI SuperNet sites, and exploring ways of increasing the bandwidth and usability of these interconnections.

1.2 Task 2: Hierarchical Multiplexing

The hierarchical multiplexing task breaks new ground, going beyond the original MONET vision. We ask: how can bandwidth be organized so that it can be used most effectively in a transparent reconfigurable network? The answer is unlikely to be the same in such a network as it is, for example, in long haul point to point transmission. The costs and impairments associated with the network elements confer different benefits and expenses. In this task we are investigating hierarchical (nested & multilevel) multiplexing rather than a “flat” approach of simply adding additional channels with finer wavelength granularity. Our contract goal was to:

- Demonstrate spectrally-efficient hierarchical multiplexing between two nodes of the MONET/ATDNet network. Possible multiplexing technologies to be demonstrated include ultra-dense wavelength division multiplexing (UDWDM), optical time division multiplexing (OTDM), optical code division multiplexing (OCDM), and frequency division multiplexing/subcarrier multiplexing (FDM/SCM).

As will be seen, we have considered each of the above multiplexing technologies, and have demonstrated spectrally efficient hierarchical multiplexing over multiple nodes.

1.3 Summary of accomplishments

During the period of the project we have accomplished essentially all of the above goals. A few highlights:

- Network stability: We have learned how the interaction of fiber and network elements create instabilities even when the network is in a static configuration, and understand how to prevent such instabilities.
- Network dynamics: We have characterized the dynamic behavior of the network during network reconfiguration, channel add/drop, in the presence of bursty traffic with varying frequency content, and in the presence of traffic with intermittent optical power dropouts. Using a combination of experiment and simulation, we have shown why and under what conditions the network experiences instability in the presence of optical power changes. We have demonstrated means to stabilize the network in each of these cases.
- Hierarchical multiplexing: We have built prototypes for two forms of hierarchical multiplexing: subcarrier multiplexing and wavebanding. We have tested each of these on

the DC Network and/or on the Telcordia NJ Testbed. We have demonstrated spectrally efficient transmission of 40 Gb/s in a single channel of the MONET/ATDNet DC Network, using a channel originally designed to support 2.5 Gb/s.

2 Task 1 Results

2.1 Network maintenance and NC&M for experiment support

2.1.1 DCN Maintenance

In the first Quarter, Telcordia checked the status of the DCN at each of the agencies, and adjusted some power levels to optimize performance. We investigated the possibility of a service contract for the ATM switches and discussed this option with counterparts at LTS and DISA. We came to the conclusion that the high reliability of the switches and the relatively low cost of replacing parts make it more cost effective not to have a service contract.

Over the following two years we continued to check the status of the DCN periodically. While we were prepared to respond to any requests for assistance, none every came. This portion of the network was stable and reliable and continues to be so.

2.1.2 Network Control and Management: Maintenance and Experimental support

During the quarter from June through August 2000 two significant improvements were made to the MONET NC&M system. In the past the NC&M system had to know about the health (availability) of **all** of the MONET network elements. If any of the network elements were not available, the NC&M system would not come up properly. This was a critical problem because of the rather high instability of the MONET physical network. The mechanism for discovering failed network elements was clumsy and difficult. Then when a failed element was discovered a configuration file had to be edited. The editing process was also difficult. (Of course when a network element returned to health this process had to be reversed.)

In the MONET system each network element has associated with it an NC&M process called an “agent”. This process acts as the “broker” between the network element and the rest of the MONET NC&M system. The architecture is illustrated in the figure on the following page.

As the figure illustrates, each agent communicates with the network element controller software via a socket. Based on this, there are two ways in which a network element may fail:

1. The element may be “completely” down – i.e. in a state where the operating system is not even functioning.
2. The element may be up but the controller software may not be running.

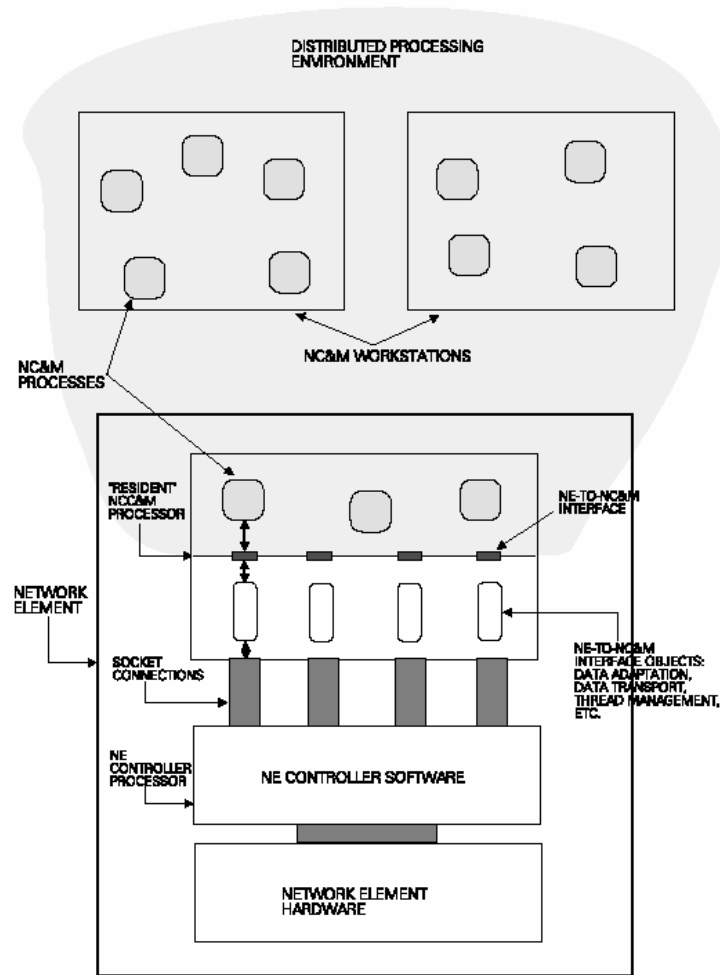


Figure 2 Schematic picture of the relationship between network management and network elements

When an agent first comes up it attempts to build a socket connection the network element. If the element is in the first of the above states this will fail.

To deal with these problems, code was added to first send a number of pings to the NE. If the responses fall below some threshold the agent knows the NE is in state 1 above. If the socket connection succeeds, the agent will attempt to connect to the controller software. If this is not running, timeout code has been added to the agent to detect this situation. In either case the agent will report to the NC&M system that an “empty” network element (i.e. an element with no shelves) exists at this site. This special empty element will be displayed by the GUI in the color blue. Any attempt to access this element will result in an error message to the user. All links associated with this element will be removed from the display. These enhancements allow the NC&M system to come up in any network configuration, and also allows the user to quickly see the state of the network.

Throughout the first half of the project, repeated visits were made to LTS and other sites to train the people there and others using the network in the use of the NC&M. Despite this training, the

NC&M system was not always used effectively, and in many cases people chose to use the craft interfaces provided by the Network Elements.

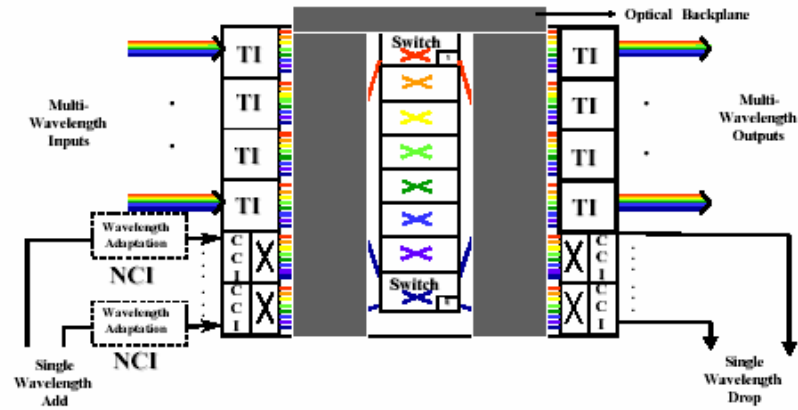
→ This points out a basic truth about management (and any other) systems: ease of use is critical. Even though the full NC&M provided more information than the craft interfaces, people chose to use the craft interfaces because they were easier to use for the most common functions of setting up and tearing down connections. Though neither the NC&M nor the craft interface could be considered “intuitive,” the craft interfaces proved easier to use, and consequently they *were* used.

One upgrade to the NC&M did find use and proved extremely valuable for the researchers. This was the provision of a set of network configuration scripts which allow the research team to set up and/or tear down a series of connections with precise timing. This capability enabled the team to make many of the measurements of network dynamics that are described below. While the scripts were difficult to write, they were well supported by the person who wrote them, were relatively simple to modify, and they provided a functionality that could not be obtained in any other way. Consequently, they were used.

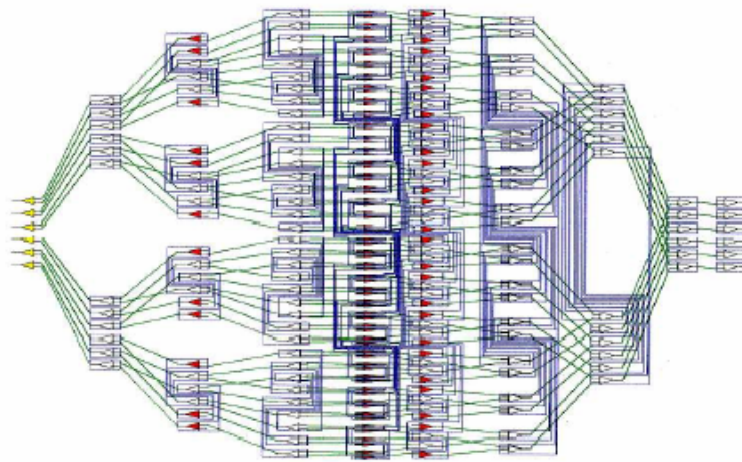
2.2 Network experiments

During the first part of this project the network was essentially that which had been built during the MONET Project, i.e., there were six agencies connected in a double ring, with network elements provided by Lucent at NSA, NASA, and NRL and by Tellium at DISA, DARPA, and DIA. During the past two years, however, the network has evolved, in part because of failures in the original equipment and in part because the agencies involved are obtaining and using new network elements. The evolution of the network allows us to generalize much of our understanding. Rather than looking at behaviors that are specific to the MONET hardware, by repeating experiments with the new network elements we can separate those effects that are the result of how the MONET NE's were designed and built from those that are more universally properties of transparent and reconfigurable networks.

The old network elements include those from Lucent, with the switch fabric based on Lithium Niobate, and those from Tellium, with an electronic switch fabric. Figure 3 a & b show the Lucent Network Element. The over-all structure of this network element is shown in Figure 3a. The multiwavelength input from each network fiber enters a TI (transport interface) where it is amplified in an EDFA and then split into the 8 wavelengths, each of which is routed to its own switch fabric. At the output, all wavelengths are combined in an output TI and the combined set of wavelength channels is amplified in another EDFA. The TI's also contain monitors for each optical wavelength, and provide information about optical power and optical signal to noise ratio at various points in the TI.. This basic structure is shared in the Tellium Network element (Figure 4). As shown, these network elements perform OEO regeneration on all inputs, but it is also possible to configure them to have a transparent bypass of the electronic switch fabric and thus optically transparent paths can be formed in the West Ring.



a.



b.

Figure 3 *The Lucent Network Element, showing (a) overall architecture, and (b) architecture of the Lithium Niobate switch fabric.*

The Tellium Network Element supports OC-3, OC-12, and OC-48 with 3R regeneration, and can also support an arbitrary digital rate up to about 2.5 Gb/s with 2R regeneration. This feature allows non-SONET traffic, like HDTV to pass through this Network Element.

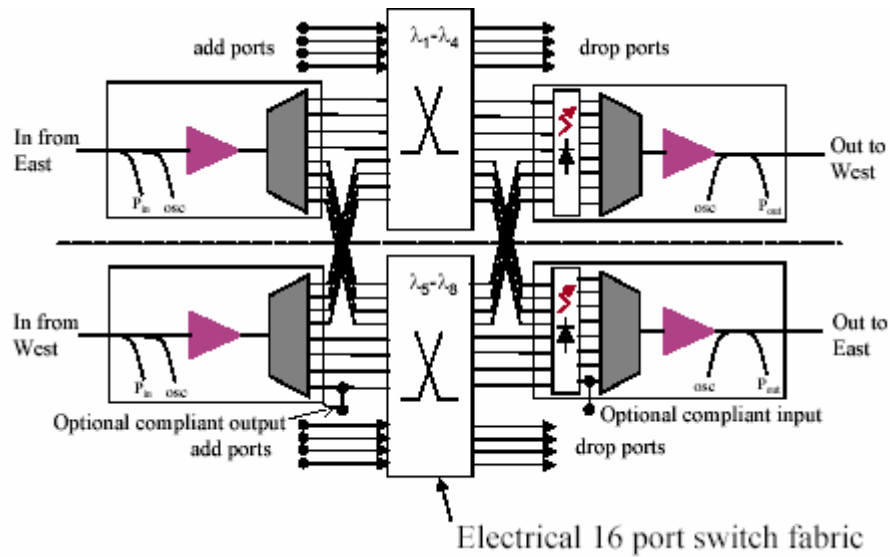


Figure 4 Tellium Network element as described in the text

2.2.1 Transmission experiments

High speeds: Most of the work on transmission at rates greater than 10 Gbps was done by the group of Professor Gary Carter of UMBC (NGI project on “High Performance Local Area Networks”) who accessed the DC Network through the LTS laboratory. We leave the reports of this work to Dr. Carter. In general the issues for high speed transmission were unsurprising. Dispersion compensation was important, but even for 20 Gbps, polarization modal dispersion was not significant for the short distances of this network. One behavior that might not have been predicted is the instability that was sometimes seen in the eye. Dr. Carter has noted two things that are of importance for this network. First it was difficult to get low BER for 40 Gbps data, probably because of polarization effects. We believe that this is related to the network instabilities discussed below. He also found that transmission of high speed data over BOSSNet was degraded when only a single wavelength channel was present; because BOSSNet does not have the per-channel optical power control of ATDNet, optical power is high when a single channel is present and consequently optical nonlinearities degrade the eye and BER performance.

Comment: The fiber in place during most of this work was old SMF-28 or the equivalent, and PMD characterization showed sections with high PMD and possibly high sensitivity to environmental effects, as seen below. Recently more modern fiber (nonzero dispersion shifted) is replacing the older fiber, and high data rate experiments should be repeated and extended to higher rates.

HDTV: The primary non-SONET data that was sent over this network is the uncompressed HDTV at 1.485 Gbps. While an optically transparent network designed for OC-48 transmission is not expected to have problems with this rate, there are two potential problems for this network.

In the West Ring, the limits come from the Tellium Network Elements, which are not truly transparent. These Network Elements regenerate everything that passes through them, with 3R regeneration for OC-3, OC-12 and OC-48. There is also an option for 2R regeneration, with no

rate specified but with a maximum rate close to that for OC-48. When the 2R regeneration mode is chosen, the HDTV signals can pass through the West Ring, though the total number of network elements that can be traversed is limited by jitter.

In the East Ring the limitations come from the optical amplifiers. Almost all HDTV traffic is transmitted successfully, but in some cases there are excess errors. The pattern that most notably causes errors is the "SIF-EQ" test pattern, which appears on the screen as solid magenta. The SIF-EQ test pattern contains periodic sequences of 19 zeros and a single one, repeating for about 17 μ s. The result is a 17 μ s period with only 5% ones, giving about 10% of the average optical power during that period. When this pattern passes through the East Ring optical amplifiers, their transient response generates large optical power swings in the HDTV channel; these are enough to degrade the received video, in some cases leading to loss of lines or even of frames. Neighboring channels are also degraded, although not necessarily as badly. More details of the SIF-EQ problem will be discussed below in the section on network dynamics.

2.2.2 Network stability

Questions of network stability arise because of the observations of "error storms" during OC-192 BER measurements. Typically, acceptable BER performance was obtained for transmission of OC-192 between nodes, and even around the entire ring, but the acceptable performance was interrupted by periods of much higher BER. Much of the first few months of this Project was spent identifying the source of these error storms. The Quarterly Reports provide a detailed chronicle of the process of tracking down the causes. A few highlight and a conclusion:

During the first Quarter we observed time-varying noise on ostensibly CW light propagating through the network. We investigated the source of the noise and found that noise builds up on CW signals from our laser sources as we concatenate network elements, but that spectrally-sliced ASE shows no such build-up.

The plots in Figure 5 show that for laser sources the noise grows rapidly as path lengths and number of network elements traversed increases. However, for ASE, there is only a slight increase in noise as paths grow. This dependence on source coherence points to multipath interference as the likely cause of noise increases. Further measurements in which a switch pack for a particular set of wavelengths was replaced with a "pseudo- switch pack," i.e., a jumper plus the appropriate attenuation, strongly suggested that the source of the multipath interference was the Lithium Niobate switch matrix.

At that time we considered that the observed noise might be the source of error "storms" that had been observed in high speed transmission experiments, but there was no clear evidence of its time dependence, nor was there a obvious mechanism for generating time varying noise levels.

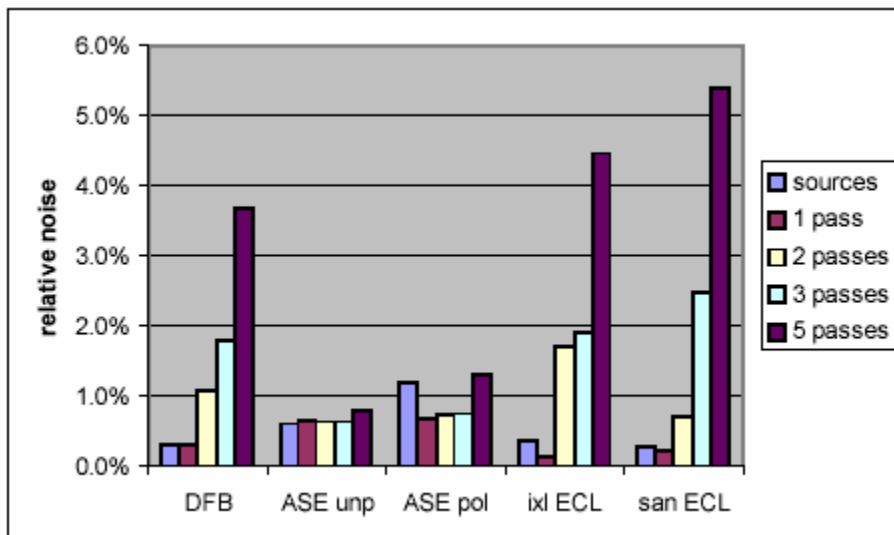


Figure 5 *Relative noise from several sources. Note that noise from ASE, whether polarized or unpolarized, does not build as a larger number of network elements are traversed. Noise builds rapidly due to multipath interference when the source is highly coherent.*

In the second and following Quarters we looked at crosstalk in the Lithium Niobate switches and correlated it with the noise. During this investigation we characterized the crosstalk for several wavelength planes at LTS and demonstrated that crosstalk levels were different in different wavelength planes, which is not surprising since the switch fabrics were experimental prototypes and each has slightly different performance. Within each wavelength plane, crosstalk depends on signal path, switch states, and polarization. A separate report, “Crosstalk Measurements at LTS,” describing some of these measurements, was attached to the second Quarterly Report and is added here as an appendix.

We have also shown more directly (a) that the observed noise is due both to multipath interference of the signal with itself in the switch fabric and to interference with other inputs in the same wavelength channel, (b) that the noise is dependent on polarization both through the polarization dependence of the crosstalk and because coherent interference takes place only for inputs having the same polarization state, and (c) that these effect lead to time-varying BER degradation, which we can produce at will. These results also enable us to prescribe methods to reduce BER penalties for high speed transmission: when possible choose a wavelength with low crosstalk on the transmission path, and select switch states having low crosstalk. During this period we continued to make measurements to identify appropriate paths and wavelengths.

More recently, as new Network Elements with different switch matrix technologies have been placed in the network, we see the multipath interference problem disappearing. The Lithium Niobate switches had such high crosstalk that multipath interference reached levels that would affect BER. The new switch matrices, based on 2D MEMS (First Wave) or on liquid crystal switches (Marconi) have much lower crosstalk and almost no polarization dependent loss, and consequently the error storm problem has disappeared.

To compare the effects of self interference of the signal with multipath leakage and interference

of the signal and other inputs in the same wavelength channel, we constructed paths with multiple passes of the signal through the same network element or with multiple passes of a second source in the same wavelength channel. We were able to eliminate the effect of the second source by offsetting wavelengths enough that the difference frequency lies outside the receiver bandwidth. Figure 6 shows a spectrum of signal and crosstalk, both within a single wavelength channel, separated by about 0.5 nm.

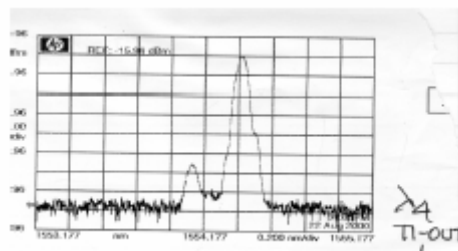


Figure 6 Crosstalk and signal in channel 4, offset from each other by about 0.5 nm.

With this kind of independent control of the signal and crosstalk wavelength and relative power, we can demonstrate several important but unsurprising results. When the signal and crosstalk separation is greater than the bandwidth of the receiver, the interference between them is minimal, but when signal and crosstalk separation is less than the bandwidth of the receiver, coherent interference gives a greater penalty. This can be seen in Figure 7 where the receiver bandwidth is approximately 30 GHz. When signal and crosstalk are separated by 0.2 nm (25 GHz) interference is much greater than when signal and crosstalk are separated by 0.3 nm (37 GHz). Of course when the source of interference is the signal itself (multipath interference) interference is *always* within the bandwidth of the receiver.

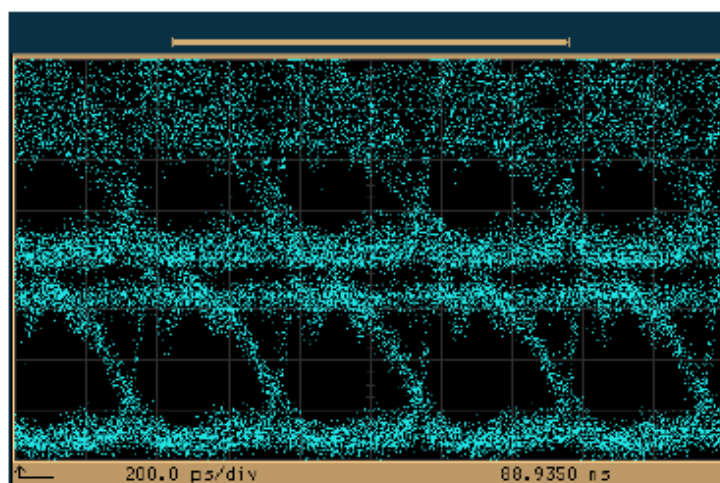


Figure 7 Upper trace shows signal sent from NSA to NASA and back, with crosstalk from signal originating at DARPA separated from monitored signal by 0.2 nm. Crosstalk generating signal is sent twice through the NE in order to maximize effect. Lower trace shows returned signal with same crosstalk, but separated from signal by 0.3 nm. In both cases polarization of incoming signal has been tuned to give maximum impairment.

Relative polarization of signal and crosstalk are also important for coherent interference. If crosstalk has the same polarization as the signal, interference is maximum; when polarizations are orthogonal, the crosstalk contributes incoherently (addition of intensities rather than addition of amplitudes) even when the difference between signal and crosstalk wavelengths is within the receiver bandwidth. Figure 8 shows this.

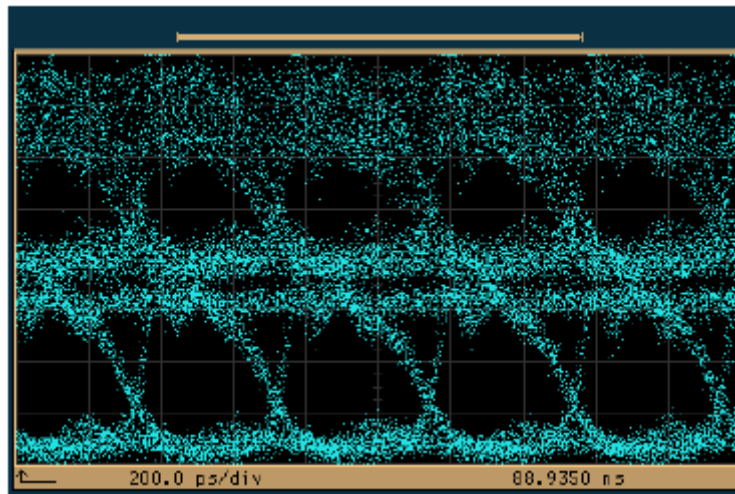


Figure 8 Signal and crosstalk as above, separated by 0.2 nm. Polarization of signal manipulated to produce maximum (upper trace) or minimum (lower trace) effect on eye pattern.

Measurements on wavelength 5, which had higher levels of crosstalk than other wavelengths in the Lucent NE at LTS, show that adding one crosstalk generator on certain input ports could increase BER by orders of magnitude.

The polarization dependence of the effect of crosstalk can easily lead to the intermittent error storms that have been observed in the past. When the polarization of a large crosstalk component aligns with that of the signal, errors can be high. Since input polarizations vary in time, BER can be expected to also. Eliminating this problem in future networks requires better crosstalk control. For measurements in the current network, the best approach is to choose wavelengths, paths, and switch states that minimize crosstalk.

The final question that these measurements forces us to ask is: What is the source of the polarization variations? The answer comes from a set of measurements made at LTS and NRL, but supported by another project. Measurements of PDL and DGD made on fiber running from LTS to DARPA-ISI show relatively stable and low values most of the time, with short periods of very high polarization effects. (Ref: C. J. K Richardson, R. J. Runser, M. Goodman, and L. Mercer, "Statistical evaluation of polarization dependent losses and polarization-mod dispersion in an installed fiber network," in National Institute of Standards and Technology Special Publication 988, Technical Digest: Symposium on Optical Fiber Measurements, 2002) The measurements indicate that periods of high DGD and other polarization effects are correlated with wind gusting. We have speculated that wind loading on fiber that is going over a bridge or an overpass may be responsible for the observed correlation.

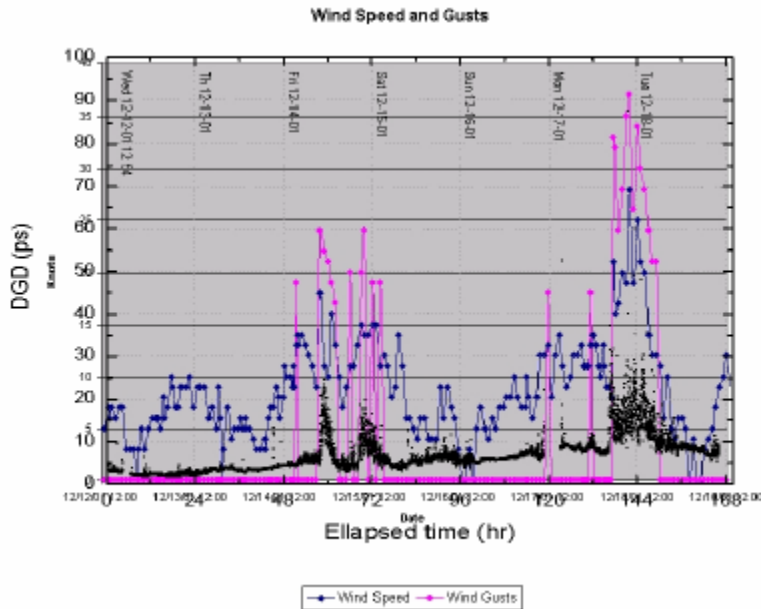


Figure 9 Measured correlation of DGD, wind speed, and wind gusting for a span of fiber

2.2.3 Network Dynamics

Much of the work in the experimental portion of the MONET Project was spent in exploring the networks dynamic behavior in the presence of bursty input, but the few months allowed for experiments during this project left many questions unanswered and, in fact, many unasked. During the MONET Follow On Project we have looked in more detail at the dynamics of the network. We have challenged the network with various types of transient events:

- Rapid network reconfiguration, including the adding or dropping of channels
- Bursty input optical power, with a variety of time scales
- Input optical data with intrinsic power variations

We note also that a network may encounter optical power changes during channel provisioning, fiber cuts, and protection switching. Provisioning, which is planned, can be engineered to minimize transients. Fiber cuts, on the other hand, are completely unplanned, and can occur on time scales rapid enough to challenge the network's ability to respond.

The original MONET network elements were designed to provide appropriate perchannel power levels regardless of the number of channels, from none to all eight. The two types of Network Elements, however, used very different forms of gain control to accomplish this, and in doing so provided response times that differed by orders of magnitude. As a result, the Lucent NE's, which were capable of microsecond reconfiguration times, had millisecond response to optical power changes, while the Tellium NE's, which reconfigure more slowly and where the OEO regeneration makes it possible to have optical power in all channels at all times, have EDFA's with a much faster (tens of microseconds) response to changing input power. I.e., the NE's that

need fast gain control do not have it and those that have it do not need it.

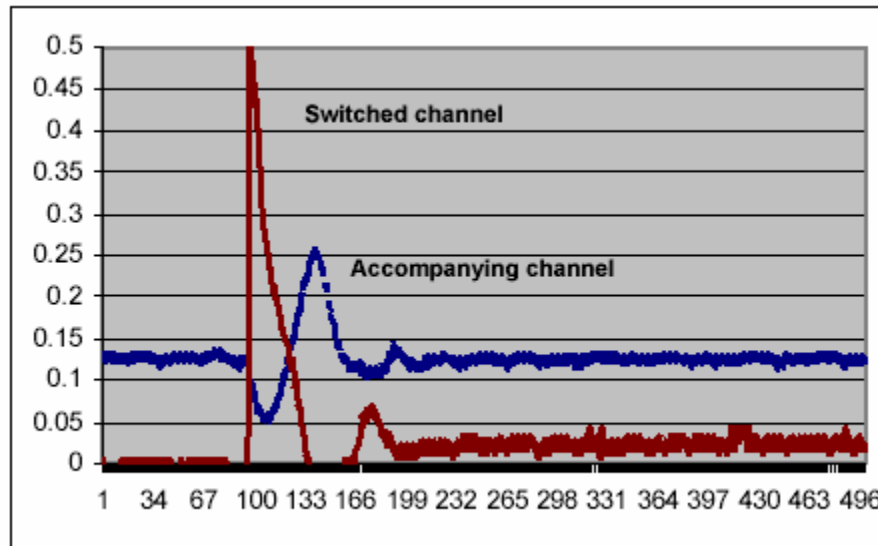


Figure 10 Switched channel and accompanying channel after NSA-NRL-NSA. Two channels have are shown on different scales; actual CW power in each is approximately equal . Total time is 500 μ s.

The replacement of the Lucent NE's with Firstwave equipment during the past year has not greatly changed the situation. These NE's have a switch fabric based on MEMS and therefore reconfigure much more slowly than the Lucent NE's, but they still have undesirable transient response when input optical power is varying rapidly.

Behavior of Lucent NE's during rapid reconfiguration Even assuming that all inputs to the network have constant average optical power, with no power variations on a time scale affecting optical amplifiers, reconfiguration, such as adding or dropping a channel, creates optical power transients. Channel adding was measured to require about 5 μ s and channel dropping less than 1 μ s. (Different choices of add and drop ports might have given different times.) Both of these times are fast compared with the EDFA dynamic response, and consequently adding or dropping a channel can create the same kind of optical power oscillations seen when a power burst is introduced through a CCI-IN. Figure 10 shows such an event for a nearly fully loaded network (7 channels going to NRL and 8 returning) when a single channel is added using the LiNbO₃ cross-connect under software control and sent to NRL and back.

When a software script was used to make and break the connection periodically, errors could be seen on at least some of the accompanying channels. Error bursts with the same period as the connection change were seen on HDTV video which shared only the NRL to NSA leg with the added/dropped channel. Video sent from NRL and back was almost completely disrupted. When a very long period was used it was possible to distinguish adding and dropping events; a single bystander channel was monitored, and small numbers of SONET errors were seen at the time of channel adding, with many few errors at channel drop. Some channels were relatively unaffected by channel add/drop. These measurements show that in the MONET network reconfiguration of the Lucent NE alone can cause errors on bystander channels, with some channels affected more

than others.

It was not possible to repeat these experiments on the EDFA's in the Tellium NE's since they produce a stay alive signal when channels are dropped and thus there is never a rapid variation of optical power during reconfiguration. However, measurements on similar EDFA's show only a small power penalty for adding and dropping seven of eight channels.

Burst transmission experiments

A wide range of burst transmission measurements have been carried out over the course of the Project. Initially we used a chopper to create bursts, but this had a limited speed, with on/off times of at least ten microseconds, and the burst length and on/off time are tied to each other. Later we used a LiNbO₃ modulator to create bursts with essentially instantaneous on/off and burst lengths that could be varied over orders of magnitude. However, the finite extinction of the modulator made it impossible to have a completely zero optical input. Both of these provided bursty optical power, but not bursty data. Finally, we built a burst generator and receiver with instantaneous (bit period) on/off, adjustable burst length and duty cycle, and pseudo-random bit streams. The data shown below came from different periods of this project, and thus different burst generators were used. We also measured the response of the network to the HDTV "SIF-EQ" test pattern, which has a naturally occurring optical power dropout of about 17 μ s.

During this time we developed and demonstrated two forms of "burst support" to prevent undesired network response to transients.

EDFA response to bursty input: In early measurements on the Lucent NE's, optical power bursts were created by passing CW optical power through a LiNbO₃ modulator. Extinction is less than total; usually a few percent of the optical power leaks through when the modulator is in the "off" state. We looked at the modulated channel alone, after it passed through two EDFA's (CCI-IN and CCI-OUT) at also after it had passed through two single wavelength EDFA's (CCI-IN and CCI-OUT) plus six common EDFAs, TI-OUT at NSA, WAMP, TI-IN at NRL, TI-OUT at NRL, WAMP, and TI-IN at NSA. Even after the two single wavelength EDFA's, the optical power transient has become distorted (Fig. 11) and after passing through the network (Fig. 12-13) the distortion is greater. Figure 12 shows the effect of channel loading; impairment is greatest when the fewest number of channels are present and is least when all channels are present in the common EDFA's. The modulated channel strongly affects accompanying channels, as Figure 13 shows, and the impairment on the bystander channel is greatest just after the power in the modulated channel increases.

The lessons learned from these results can be supplemented by early measurements during the experiments phase of the MONET project, where similar results were obtained, but primarily for slower changes in the optical power. There it was found that slower changes in power created smaller impairments than faster changes, and that higher input power for the optical power burst created larger impairments than smaller input powers. The second of these observations is also supported by our measurements on inputs similar to the SIF-EQ video test pattern.

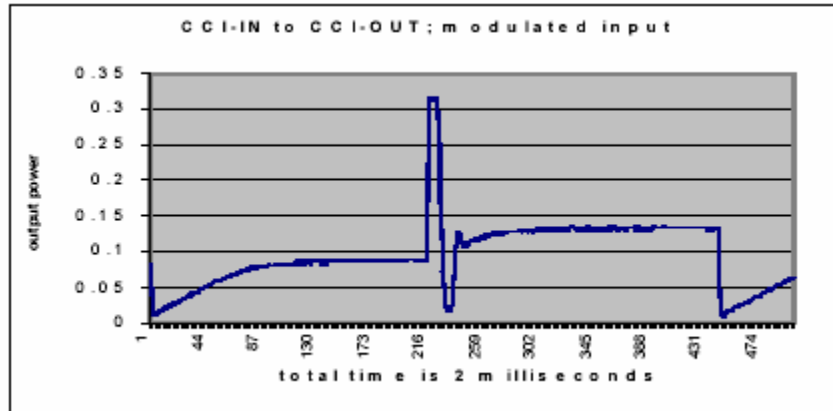


Figure 11 Output of CCI-OUT for a CCI-IN to CCI-OUT path (power added and dropped in the same NE without passing into the network) for a modulated input. Because modulation is less than 100%, EDFA gain increases during "off" period.

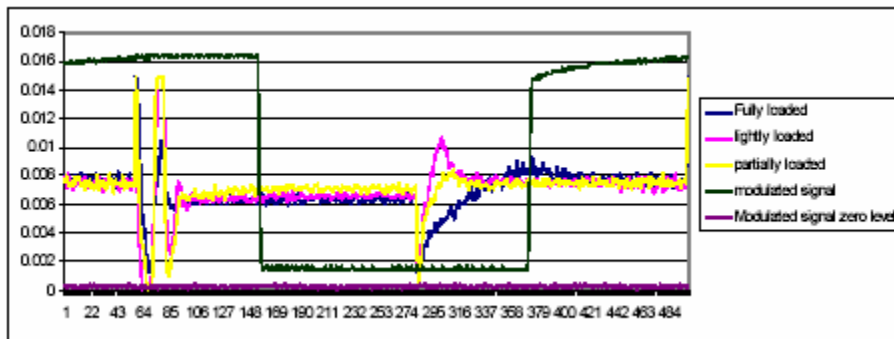


Figure 12 Modulated channel after passing through network to NRL and back to NSA: two single wavelength EDFAs and six common EDFAs. Impairment is greatest when only two channels are present (lightly loaded) than when the network is fully loaded., and for partial loading, the impairment is intermediate.

The above extreme responses to bursty input power results from the great depth of saturation of the EDFA's in the Lucent NE's. However, even less saturated EDFA's can produce responses to bursty inputs that degrade performance of the bursty data and in some cases that of accompanying channels. Measurements in the Firstwave NE's that have largely replaced the Lucent NE's over the past year show less extreme EDFA response, but still have degraded performance immediately after the burst enters the NE. Figure 14 illustrates the response of the Firstwave equipment. Bursts passing through only the client EDFA's experience much less distortion than those passing through the same part of the Lucent NE, but competition between amplifier dynamics and hardware/software driven gain control in the multichannel EDFA's can lead to unpredictable behavior, in this case a rapid drop in output power shortly after the burst begins.

Even when there is no obvious distortion of the optical power envelope, bursts do not fare well. Figure 15 shows how short bursts (total time shown is 40 μ s) with varying duty cycle emerge from a series of EDFA's. While the average power is the same in all cases, for short duty cycles,

the power in the data is much higher. This can lead to distortion due to nonlinearities for long enough transmission distances.

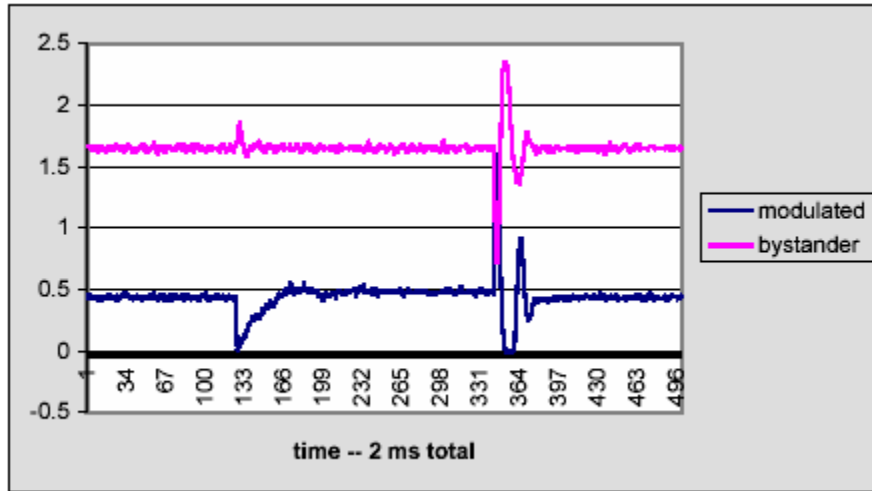


Figure 13 Power through the network for the modulated channel and a bystander channel, when only two channels are present. Impairment of the bystander channel is greater when the modulated channel enters the "on" state than when its power is decreased.

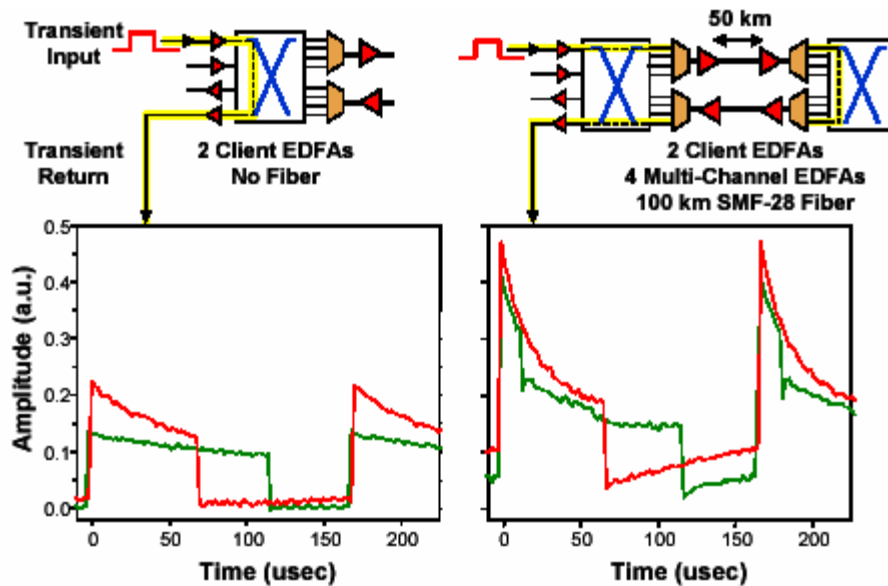


Figure 14 Bursts passing through the Firstwave NE experience much less distortion than those passing through the Lucent NE, but competition between amplifier dynamics and hardware/software driven gain control in the multichannel EDFA's can lead to unpredictable behavior

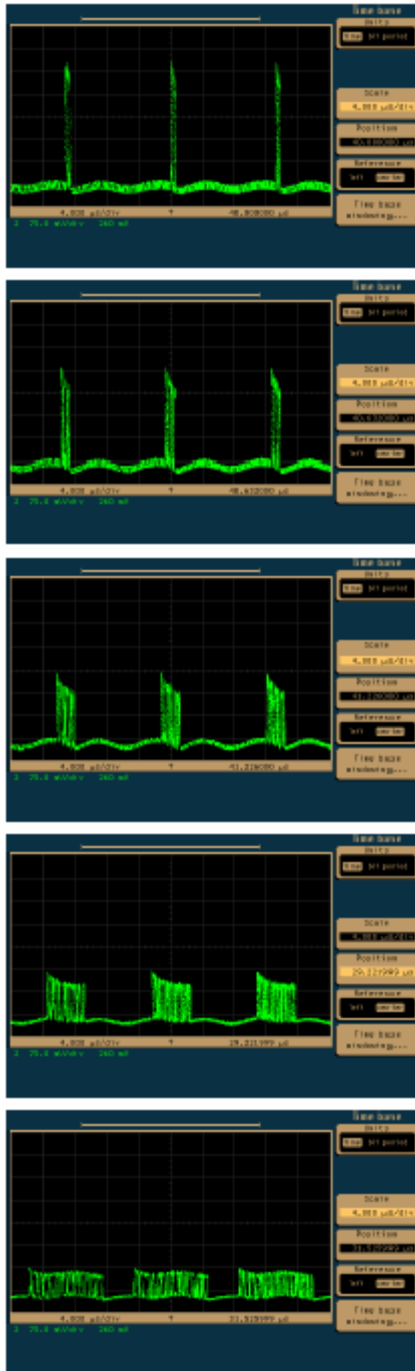


Figure 15 Bursts of varying lengths after passing through the Firstwave Network Element, as shown above.

Because of these degradations we have developed methods for stabilizing EDFA gain. To do so and to allow us to study the optical power transients, we have developed burst mode transmitters and receivers.

Burst transmitters and receivers, and burst support

Measurements of burst transmission would be impossible without burst transmitters and

receivers. Both have been developed with support from this program. The transmitters are bit-rate-agile and can generate burst of various length and with various duty cycles. The receivers are also bit-rate-agile, and can acquire clock within a few bits. These components allow us to take advantage of the transparency of the network as well as to test its performance.

With the emergence of rapidly reconfigurable WDM optical networks, many companies within the optical networking community have proposed simplification of the OSI layer stack for packet transmission which could improve performance while significantly reducing overall cost. As this will lead to transmission of packets as optical bursts sent directly over a WDM channel, we investigated this mode of transmission using the MONET DC testbed as a real-life model.

A programmable burst mode transmitter was refurbished to allow greater diversity in packet types, including means for providing both in-band and out-of-band optical burst support. In-band optical burst support utilizes substitution of a 30MHz square wave between packets to minimize variation in mean optical power. This was done by extending the lower frequency range of the burst transmitter. Out-of-band burst support utilizes substitution of a 20MHz square wave from second laser with wavelength in the data channel optical pass-band. Both methods show promise in facilitating burst transmission through an EDFA. A number of different types of optical amplifier responses were emulated on the NSA-NRL path by varying the response time of the substituted signal.

Figure 16 shows the burst mode transmitter and receiver.

WDM networks additionally offer the promise of rate and protocol transparency. We demonstrated error-free transmission of packets at variable bit rates over an NSA-NRL path using in-band optical burst support. Our receiver was able to rapidly recognize and lock onto one of three rates, 700Mb/s, 350Mb/s and 233Mb/s. This was the first network based demonstration of rate adaptive clock recovery as well as on-the-fly rate agile packet transmission. Packets having a single rates and packets having different rates for header and payload were investigated. The mixed rate packet shows great promise for in-band optical label switching and optical packet storage. These experiments dispelled concerns that jitter and other impairments would limit the usefulness of on-the-fly rate agile protocols.

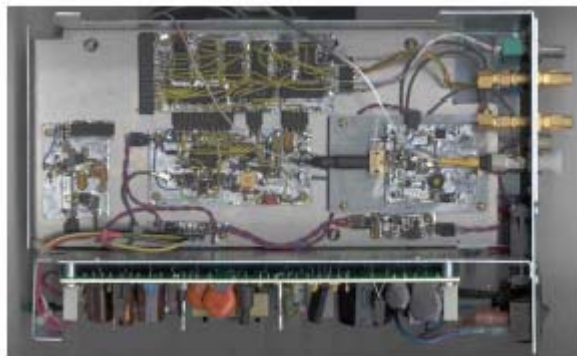


Figure 16 Burst Mode transmitter/receiver

The in-band and out-of band burst support allow bursty data to pass through the network and NE amplifiers without degradation. Figures 17 a & b illustrate the value of this type of burst support.

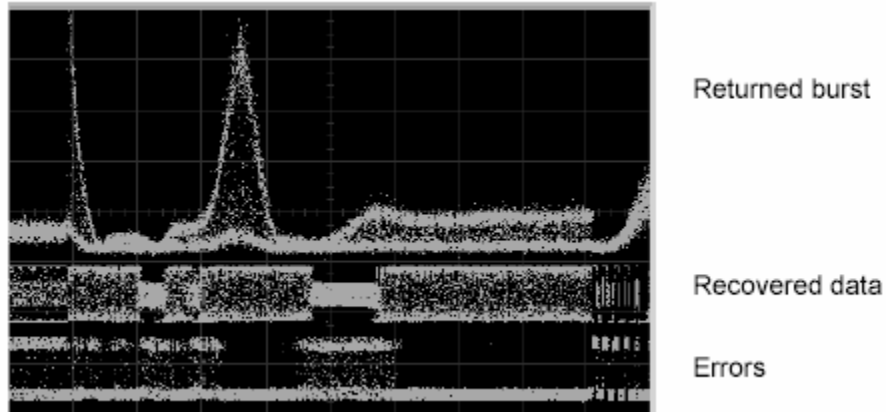


Figure 17a *Burst sent from NSA-NRL-NSA along with recovered data, and a measure of errors.*

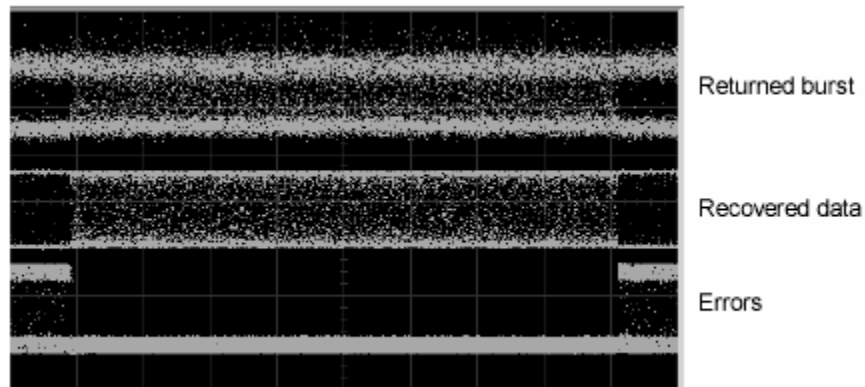


Figure 17b *Same as above, but using burst support.*

All-Optical Burst Support: The above type of burst support, in which either the laser transmitting the data burst or a second laser with wavelength lying in the same wavelength channel is used to fill in with modulated optical power during the time no burst is transmitted, can eliminate the optical power transients that otherwise occur in this network. However, this method is not useful if the bursty data is presented to the network in optical form and is not regenerated. We therefore developed an all-optical burst support method using a semiconductor optical amplifier (SOA) to generate the burst support optical power. This SOA can take the place of the input EDFA currently used in the network element CCI-IN.

All-optical burst support is accomplished by using the SOA in a saturated mode (i.e. output power is essentially independent of input power) for all expected input powers, but embedding the SOA in a feedback loop which causes the SOA to become a laser when input power drops below a certain level. If the wavelength of the laser is within the same wavelength channel as the true signal, it will propagate through the network in the same way as the signal. Thus, when a signal is present, it is amplified by the SOA to a fixed level, and when no signal is present, the SOA provides optical power to replace that which is missing. Downstream EDFAs experience

nearly constant input optical power.

Figure 18 shows (a) the SOA-laser structure and (b) both the signal and the lasing wavelength for such structure when the input at the signal wavelength is below the “nolasing” range. In this case both lie within the same wavelength channel, as can be seen by comparing the lasing and signal spectra to filtered ASE.

The burst support wavelength is generated within less than one microsecond. Figure 19 shows a short (6 μ s) burst which has taken the path CCI-IN to CCI-OUT within the Lucent NE, i.e. within a single network element it has passed through the saturated input and output amplifiers. The presence of the burst support prevents distortions of the burst itself as can be seen in Figure 20, which shows a longer burst taking the same path with and without the burst support.

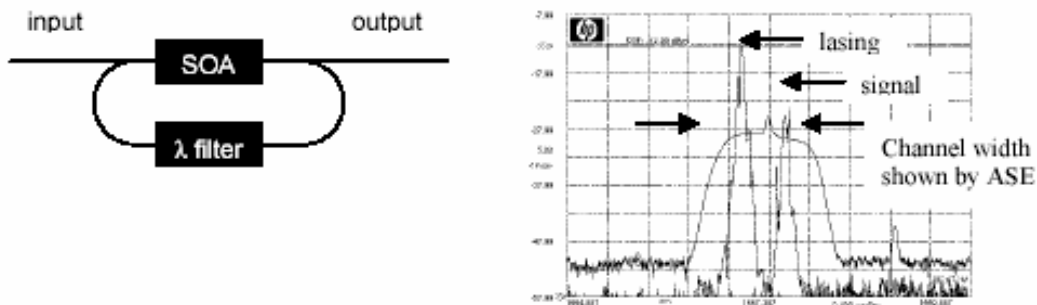


Figure 18 (left) SOA embedded in laser structure, with lasing only if input power drops below expected signal level. (right) Spectrum of combined signal and burst support wavelengths, compared with width of channel.

Preliminary measurements on the network (to NRL and back) indicate that bursts with all-optical burst support can be received error free, or nearly so, in circumstances in which unsupported bursts are heavily errored. Figure 21 shows a train of bursts which have passed through the network. The burst support eliminates nearly all errors. Without burst support initial part of each burst would be heavily errored.

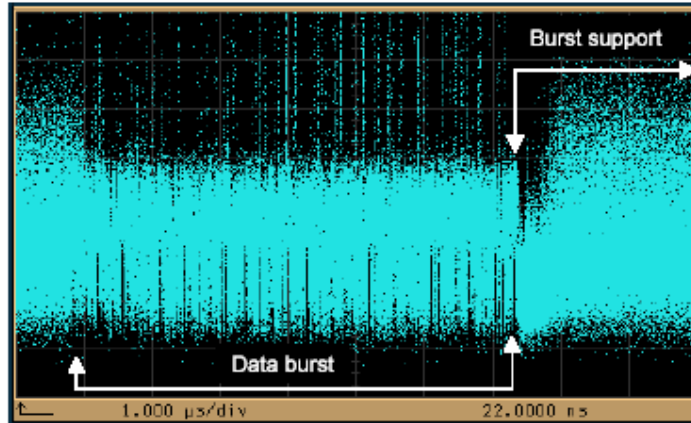


Figure 19 Data burst (in center) followed by optically generated burst support. Rise time for burst support power is less than 1 microsecond.

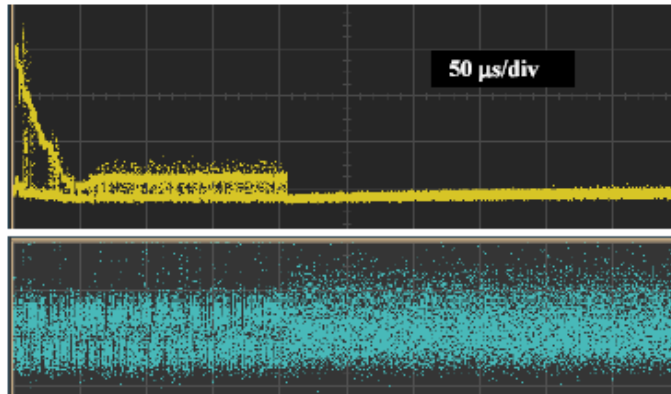


Figure 20 240 μs burst after CCI-IN to CCI-OUT path, (a) with and (b) without burst support. With burst support the burst is not distorted. In both cases the bursts occupy the same portion of the trace.

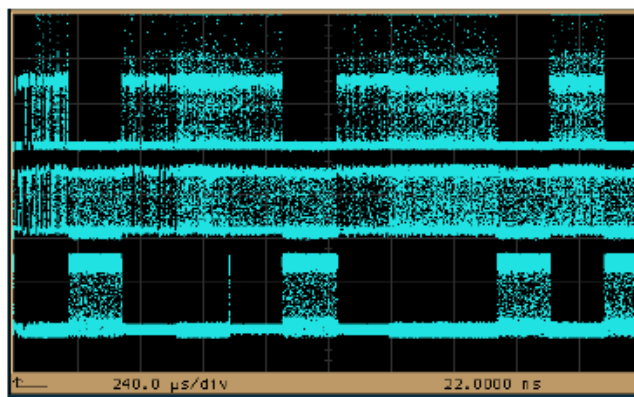


Figure 21 Multiple bursts (a) bursts generated by transmitter (b) after passing through the network, with burst support, (c) errors: low level indicates no error and high indicates error. Errors are expected when no signal is present.

A final example of the value of SOA based all-optical burst support can be seen in a simulated SIF-EQ transmission created by transmitting data with a 13 μs dropout period. Figure 22 shows returned data from a LTS-NRL-LTS path without (a) and with (b) SOA based optical burst support.

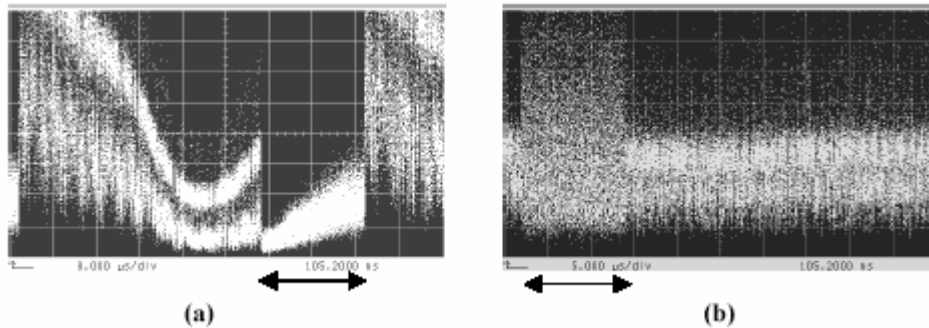


Figure 22 Returned data after path from NSA to NASA to NSA, with 13 μs dropout. (a) With no optical burst support, returned power has large swings. (b) With SOA optical burst support, returned power has no large swings. Arrows indicate period of dropout.

When SOA-OBS is used, there is optical power during the dropout period, provided by the SOA, and consequently no increased gain and optical power overshoot after the signal power return. Because there is no large optical power fluctuation, there are also no excess errors. Figure 23 presents a measure of errors; where the trace shows “1”, there is no error, and where it shows “0” there is an error. The top trace represents the errors on returned data with a dropout, with no optical burst support. In either case, errors are detected during the dropout period, since there is no data, and for a short time after the return of data, while the receiver is reacquiring the clock.

These measurements and those in the attached paper provide some guidance for next generation networks. Burst support, either the SOA-OBS reported here or the optoelectronic (regenerating) burst support described in the previous Quarterly Report, allow burst transmission in a transparent network. SOA-OBS can provide burst support at essentially any rate and for bursts of any duration and spacing; it enables an even wider range of transparency than opto-electronic burst support. For example, it allows transmission of native HDTV signals at 1.485 Gb/s, a rate which it may not be possible to regenerate with conventional circuits, and protects against degradation due to the “SIFEQ” pattern. SOA-OBS thus makes it possible for transparent optical networks initially designed only for provisioned wavelengths to transport optical power bursts without degradation.

This SOA-OBS need be provided only at the input to the network, since the presence of a complementary optical signal at a wavelength within the same wavelength channel maintains a constant input power to all the EDFAs in the burst’s path, so long as excess polarization dependent loss does not destroy the optical power balance. However, as the paper notes, polarization dependent loss within network elements can subvert optical burst support of this kind, since the polarizations of the signal and substitute wavelengths may be different at the network input and even when they are identical at the input they can drift away from each other after propagating through many kilometers of fiber.

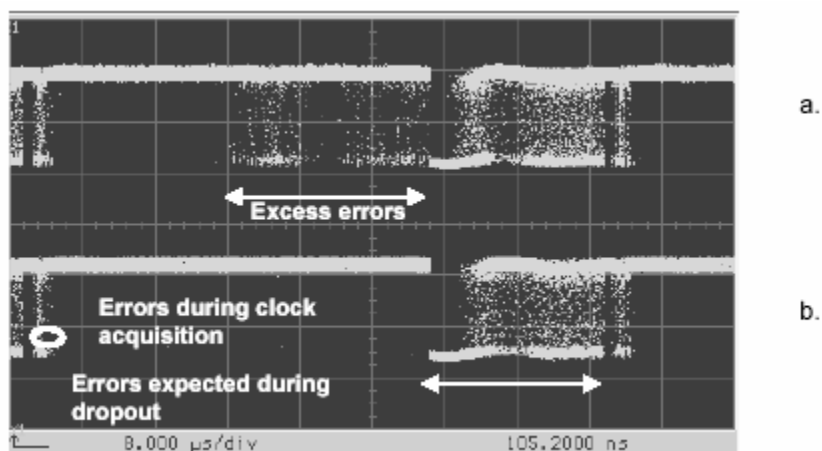


Figure 23 Errors are seen after dropout when there is no optical burst support (a) but not when SOA-OBS is used (b) Scale is 8 μ s/division

Consequently, low polarization dependent loss is a necessity in networks intended to carry data stabilized with SOA-OBS. The added stability makes this additional demand on the network.

Note also that SOA-OBS does not provide stability against optical power variations during network reconfiguration. However, most all-optical cross-connects intended to be used in reconfiguration (MEMS, bubble switches, liquid crystal based switches) have long enough reconfiguration times that existing EDFA designs, for example the alloptical gain clamping of the West Ring or a moderately faster version of the pump power gain stabilization of the East Ring, will be able to adjust to changing numbers of channels. The fast LiNbO₃ based optical cross-connect now in the East Ring of the MONET/ATDNet network has been seen to create errors in one channel when another channel sharing the same amplifiers is added, but such fast switching times are unlikely to be encountered in next generation networks using slower cross-connect technologies. (In the MONET/ATDNet network, reconfiguration times are much longer than the microsecond speed of the optical switch fabric. Software limits the actual reconfiguration to several tens of milliseconds, four orders of magnitude slower; only the optical power transition time is fast.)

On exception to this reassuring conclusion is the case of all-optical packet switching, for example the Optical Label Switching now being developed at Telcordia. In this case, fast (sub-microsecond) switching of packets can lead to optical power transients in downstream amplifiers, unless some form of burst support is used. In most versions of optical label switching now under investigation, burst support is provided, in many cases by regenerating the signal.

The improved performance obtained with burst support and with SOA-based optical burst support has been reported in

J. Jackel, T. Banwell, S. McNown, J. Perreault, "Burst Optical Transport over the MONET DC Network," ECOC 2000

J. Jackel, T. Banwell, S. McNown, J. Perreault, "All-Optical Burst Support for Optical Packets,"

ECOC 2002

which are attached to this Final Report as Appendices.

2.2.4 NC&M Experiments

NC&M Experiments were primarily those that supported other experiments, but they also provide information about the NC&M system. In creating the scripts that control the burst reconfiguration measurements, for example, we learned that the minimum software determined reconfiguration time was approximately 25 ms, although the switch fabrics themselves responded in about 1-5 microseconds.

Since NC&M experiments were eliminated in the rescope of the project, no NC&M experiments were done in the latter half of the project.

2.2.5 Other

We also helped support other experiments of interest to the Agencies connected to the network. The most noteworthy were a series of Quantum Key Distribution experiments, which are continuing with further support from one of the Agencies. We have worked to improve the connection with BOSSNet, in order to allow experiments to be carried out over the combined ATDNet/BOSSNet network. The issues in making the connection are to avoid interfering with any BOSSNet functions and to allow us to route some wavelengths to BOSSNet while maintaining the ATDNet ATM connectivity on wavelengths 3 and 4 along with the West Ring gain stabilization channel at 1545 nm.

Figure 24 shows the BOSSNet connector we have created.

The 1545 nm splitter and combiner are used to bring the Tellium gain clamping wavelength around the BossNet bypass and send it to the Tellium NE, which needs it. We could have eliminated this if what is going to DARPA is relatively stable, but it is there as a precaution.

The 2x2 switch allows us either to return to the normal connection, or to send all but wavelengths 3 & 4 to BossNet. It is set up this way, rather than with 2 switches, so that there is no need to make sure the switches were in compatible states.

The fiber Bragg gratings appear to be the best way to drop these two wavelengths. If we used interference filters, they would each come out on a separate fiber and then need to be combined. However, Fiber Bragg gratings that can drop an entire 100 GHz wide channel are difficult to manufacture. The wait for these gratings delayed the BOSSNet connector which has, however, finally been constructed and is expected to be installed within the next few days.

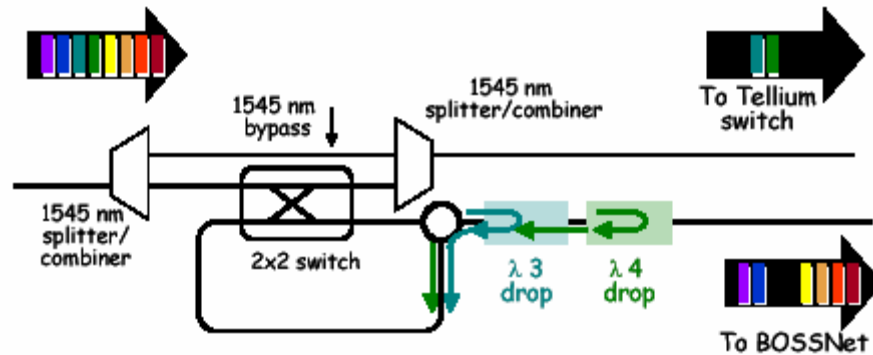


Figure 24 BossNet connection in ATDNet to BOSSNet direction

3 Task 2 Results

The Figure below summarizes our work on hierarchical multiplexing.

3.1 Why Hierarchical Multiplexing?

The basic problem is that a network of this kind that attempts to support a large amount of bandwidth needs to organize that bandwidth in some way. One way to increase bandwidth is simply to increase the number of wavelengths from the 8 that the original MONET/ATDNet network carried to much larger numbers of channels with significantly narrower channel spacing. For point to point transmission this is straightforward. However, in a reconfigurable network this creates issues in the nodes, which need to add/drop or to pass through those channels. In the MONET network we had 8 wavelengths and 6 nodes, and the network was designed to carry a bit rate of 2.5 Gb/s per channel for a total of 20 Gb/s. But the intrinsic capacity of the fiber is much greater. Since the existing channels are over 100 GHz wide, the available bandwidth per existing wavelength channel is much greater than the original 2.5 Gb/s. To take advantage of that capacity by increasing the number of channels and decreasing their spacing demands that the nodes be redesigned to be able to process each of the wavelengths, but it is clear that in a network of modest size all the bandwidth need not be independently routed. What happens, for example, when the number of channels is considerably larger than the number of nodes? Instead of expanding bandwidth in a “flat” way,, we are looking at hierarchical methods of multiplexing the bandwidth into the existing channels, in order to provide usable bandwidth that more efficiently uses the fiber’s total available bandwidth without the need for complete node redesign. This approach allows expansion of bandwidth as needed without requiring initial deployment of a more complicated (and thus more expensive) node, and allows upgrade as needed. The methods we are investigating are:

- Multiplexing to higher bit rates (10 Gb/s, which is relatively easy, and to 40 Gb/s, which is difficult due to fiber and network element dispersion and other effects). Most of the highest bit rate experiments on this network have been done by a separate group headed by Professor Gary Carter of UMBC, with whom we collaborate. However, rates up to 10 Gb/s can use this network without special engineering (see results as far back as the MONET project itself) as long as multipath interference is minimized.

- Multiplexing several wavelengths (subchannels) into a single channel. This appears straightforward, but in a reconfigurable network the sub-channels are subject to degradations not encountered in simple transmission.
- Subcarrier multiplexing
- Optical CDMA

Efforts on underway in all of these directions, and it is our intention to provide a comparison of these methods by the end of the project, along with a definition of the requirements for networks that would carry any of them. We are also interested in the extent to which any or all of these multiplexing methods could coexist on a single network.

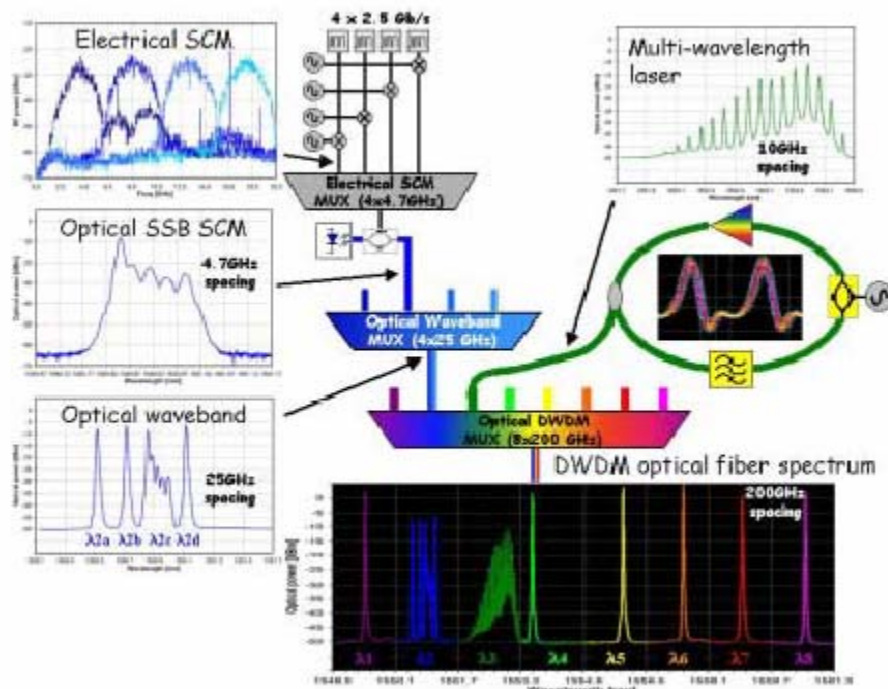


Figure 25 Summarizes work on Hierarchical Multiplexing

3.2 Hierarchical Wavelength Multiplexing

Noteworthy results in the last months of this project have included multiplexing of four 10 Gb/s subchannels onto a single MONET wavelength, for a total channel capacity of 40 Gb/s, and transmission of this data through a total of three network nodes at NRL and LTS. Unlike transmission of a single 40 Gb/s channels, this requires no high speed electronics or optical multiplexers, and it also requires only standard dispersion compensation. Error rates for this data was essentially the same as for a single 10 Gb/s channel carried on the same wavelength channel. We are now working to define the best network element design to be compatible with this and the other types of multiplexing. Figure 26 shows the four-wavelength source.

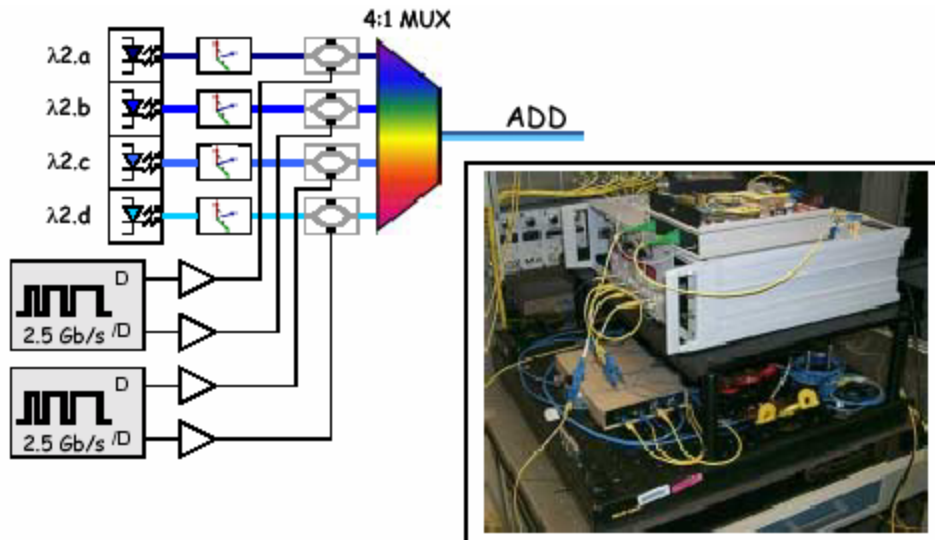


Figure 26 Source for 4 2.5 Gb/s channels carried in a single MONET wavelength channel

Four independent tunable lasers are polarization controlled and then independently modulated before being combined and added to the network through a single wavelength port. At the receive end, all 4 sub-channels are dropped through a single wavelength channel port and then demultiplexed using fiber Bragg gratings. Performance measurements were made both on the NJ MONET testbed and on the MONET/ATDNet DC network, using either the original MONET network elements built by Lucent, or replacement network elements from First Wave. In the NJ testbed and when the First Wave equipment was used in the MONET/ATDNet DC Network, BER for data sent through the network was nearly identical with back-to-back measurements. Figure 27 shows the experiment at the MONET/ATDNet LTS node, along with the inserted and dropped spectrum. The grouped sub-channels therefore pass through a total of three network elements.

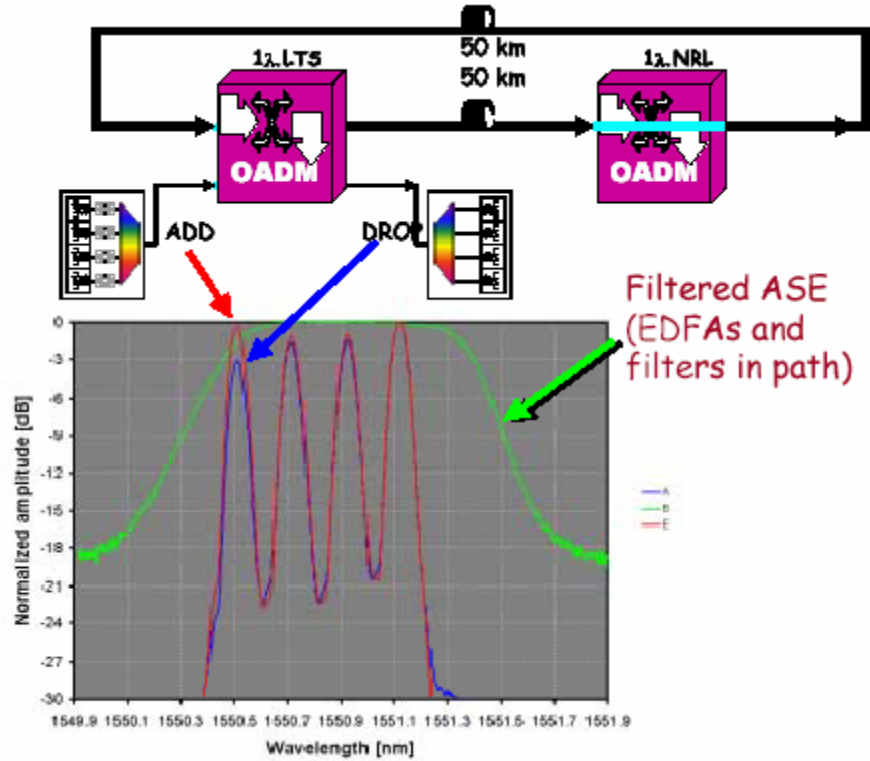


Figure 27 (a) Experiment at LTS on the MONET/ATDNet DC Network,, with four 2.5 Gb/s subchannels added at a single wavelength port, passed through the network to NRL, through the network element at NRL, and then dropped through the originating network element at LTS.

Figure 28 shows the BER for the 4 x 2.5 Gb/s experiment at the MONET/ATDNet DC Network.

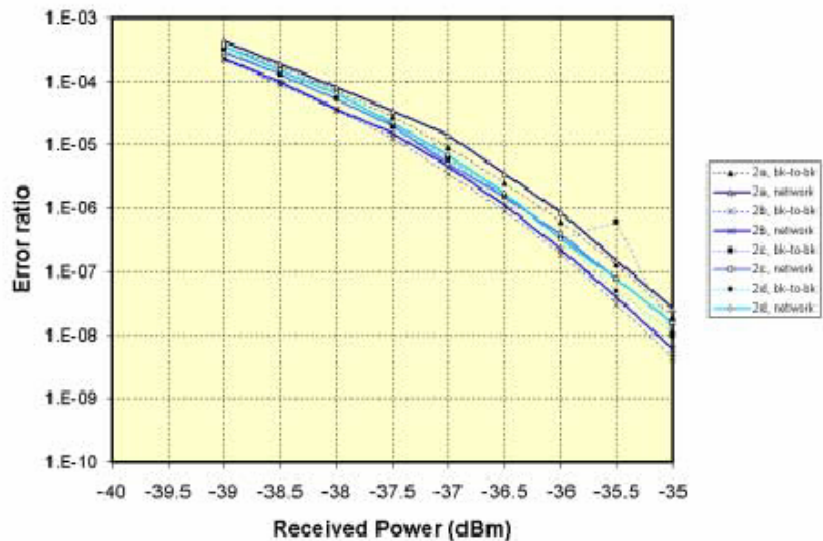


Figure 28 BER for the 4 x 2.5 Gb/s experiment at the MONET/ATDNet DC Network

Measurements were also made using 4 x 10 Gb/s sub-channels. The transmitter differed slightly from that for 4 x 2.5 Gb/s since we had only one driver/modulator pair that could function at that speed. Therefore all channels were modulated in the same modulator, as shown in Figure 28. The same measurements were made for these as for the four 2.5 Gb/s data. BER for the four channels are shown in Figure 29. For 10 Gb/s, there is a power penalty of about 1 dB for three of the four channels, and the fourth channel has a larger power penalty of about 1.7 dB at an error rate of 10^{-9} .

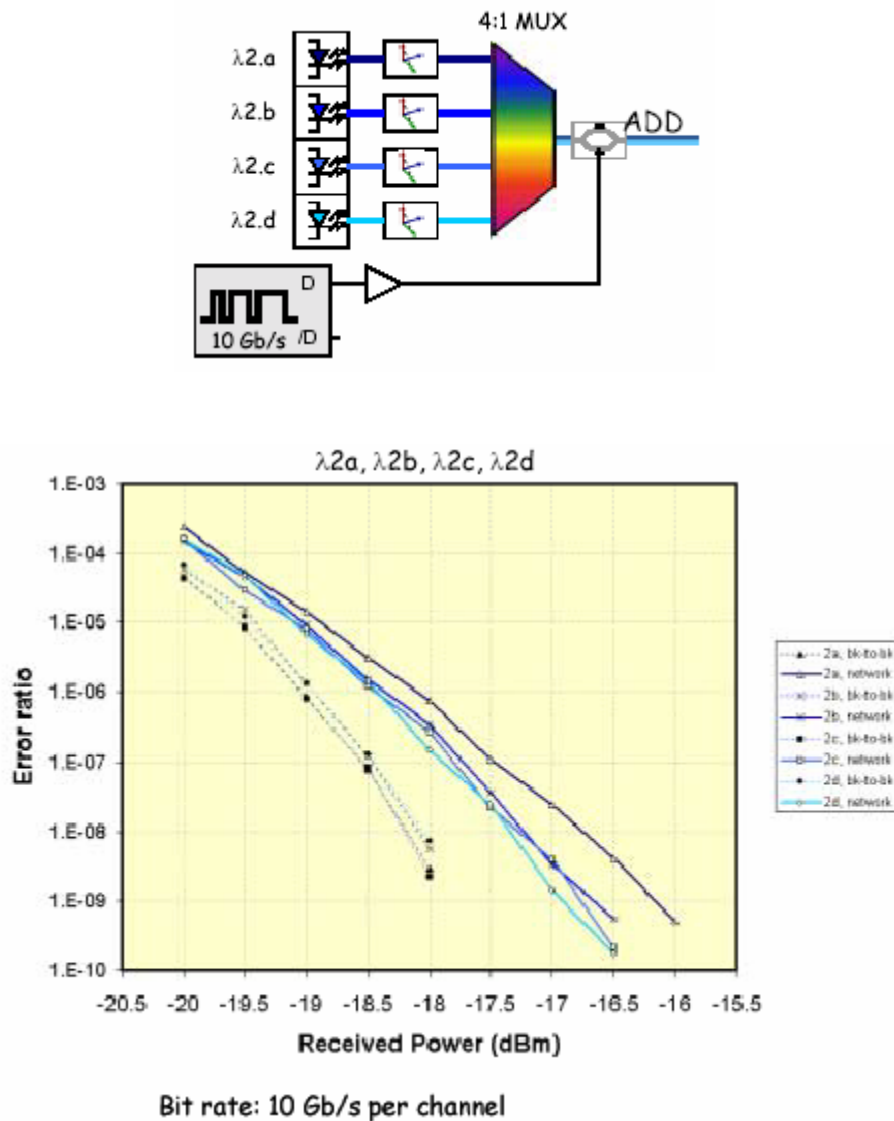


Figure 29 BER for the four channels

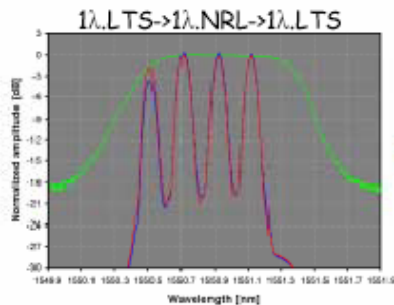
The increased power penalty for the fourth channel is one of the consequences of inserting the more closely spaced channels into a transparent reconfigurable network. Figure 27 (above) showed that while the three subchannels in the flattest part of the network element passband suffered little or no differential loss after three passes through NEs, the fourth subchannel, which lies at the edge of the passband, emerged from the network with a relative loss of about 4 dB, and therefore a reduced signal to noise ratio, which leads to higher power penalty. We also

observed that the relative loss at the edge of the passband was slightly polarization dependent.

If we compare the output spectrum for two versions of the same path through the MONET/ATDNet DC Network, as in Figure 30, one source of degradation becomes evident. As relative polarization of the subchannels changes due to their passage through the network fiber, polarization dependent loss in the network element causes their relative power to change. The Figure captures the range of variation over time, with the red trace giving the maximum power in any wavelength and the blue trace representing the minimum. In the First Wave equipment, polarization dependent loss is small, but in the Lucent equipment, which uses LiNbO₃ for its switch matrix, the range of output powers is large. This large polarization dependent loss is responsible for our previous difficulty in obtaining stable relative output powers for two wavelengths in a single channel (reported in the Quarterly Report for September 2001) and for our choice to make the error measurements using First Wave equipment. While the two types of network elements have similar architectures, they are realized using different technologies; for example, the First Wave network elements uses a MEMS switch fabric while the Lucent NE uses LiNbO₃. These differences can have major consequences when the NEs are used in ways for which they were not originally designed.

In the next few months we plan to continue these measurements with four independently modulated 10 Gb/s subchannels, and will also look at the behavior of other network element designs with subchannels.

- One notable result of the above measurements is that we have used a MONET wavelength channel originally designed to carry 2.5 Gb/s and by multiplexing subchannels we have been able to make it carry a total of 40 Gb/s, with no redesign of the node. This is one of the benefits of optical transparency, which the original MONET project was intended to investigate.



a. Maximum and minimum power in the subchannels after passing through three Firstwave NE's. Power variation is small except for the shortest subchannel (at the left) and for that subchannel, variation is about 2 dB.

b. Maximum and minimum power in the subchannels after passing through two Lucent and one Firstwave NE's. All channels experience relative power variations of 4-6 dB.

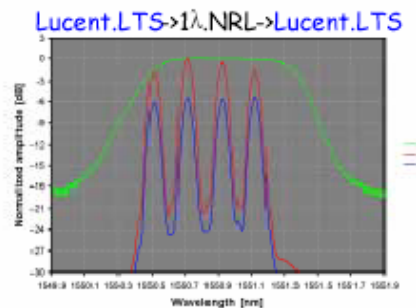


Figure 30 Comparison of output spectrum for two paths through the West Ring, one through a combination of Lucent and Firstwave NE's and the other through Firstwave NE's only.

3.3 Subcarrier Multiplexing

We have begun preliminary study of subcarrier multiplexing on a transparent reconfigurable network. At this time we have assembled a subcarrier multiplexed transmitter and receiver for four 2.5 Gb/s subchannels, and have made preliminary tests on the NJ testbed. We expect to take the transmitter/receiver to the DC Network in the next months to test behavior on the more realistic network. Figure 31 summarizes results to date.

Figure 31 Summary of SSB modulated multiplexing of multiple channels, showing the transmitter (left center) , receiver (right center), The difference between the input and output electrical spectra arises from the frequency roll off of modulation efficiency in the single optical modulator.

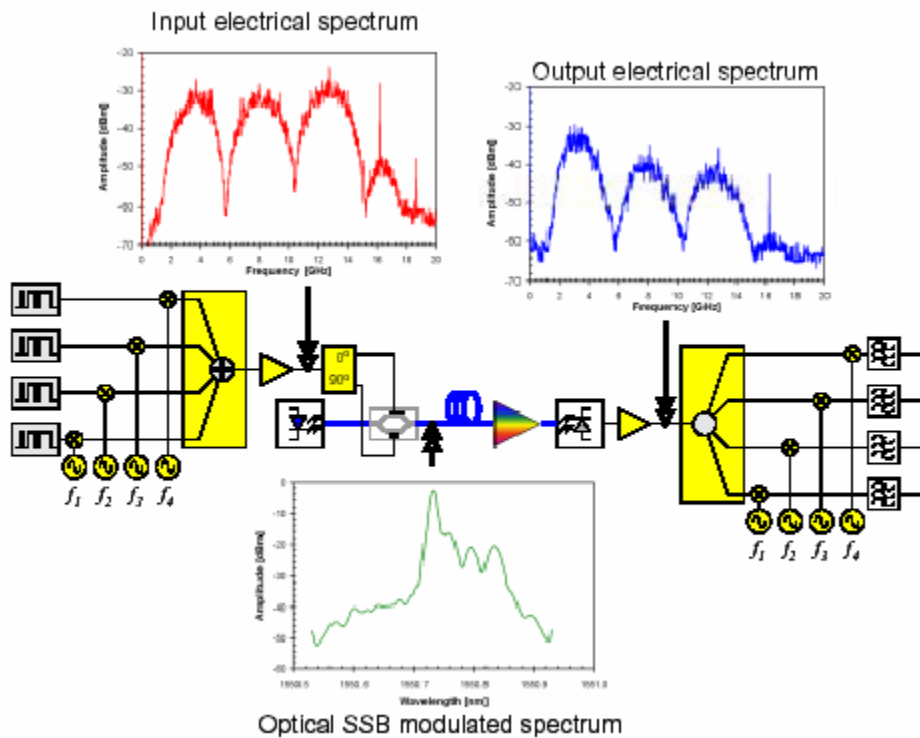


Figure 31 Summarized results to date

3.4 Multiwavelength source for Hierarchical multiplexing: wavebanding and OCDMA

We have worked in collaboration with Peter Delfyett of CREOL to develop a stable multiwavelength source suitable for use either for wavelength subchannels or for OCDMA (the

last type of hierarchical multiplexing we are addressing) within a wavelength channel. The source has been described in our earlier reports. During this Quarter we have worked to stabilize the source. Figures 32 and 33 shows the laser and a transmission experiment testing its suitability for OCDMA. The laser is within the shaded box.

Experiment Setup

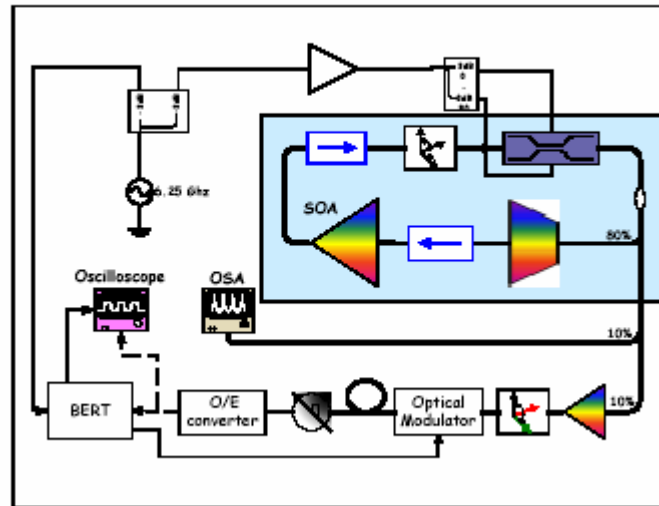


Figure 32 Modelocked laser multiwavelength source, and transmission experiment for 6.25 and 10 Gb/s. Optical portion of the laser lies within the shaded box.

Figure 33 shows the RZ data generated by this laser, the optical spectrum all of which lies within a single channel, and the BER for 6.25 and 10 Gb/s data. We continue to explore the capabilities of this source, particularly as it can be used for OCDMA. (We have also submitted a proposal in response to DARPA BAA-02-18 for OCDMA; the proposal has been accepted and we expect to begin work by December 2002.)

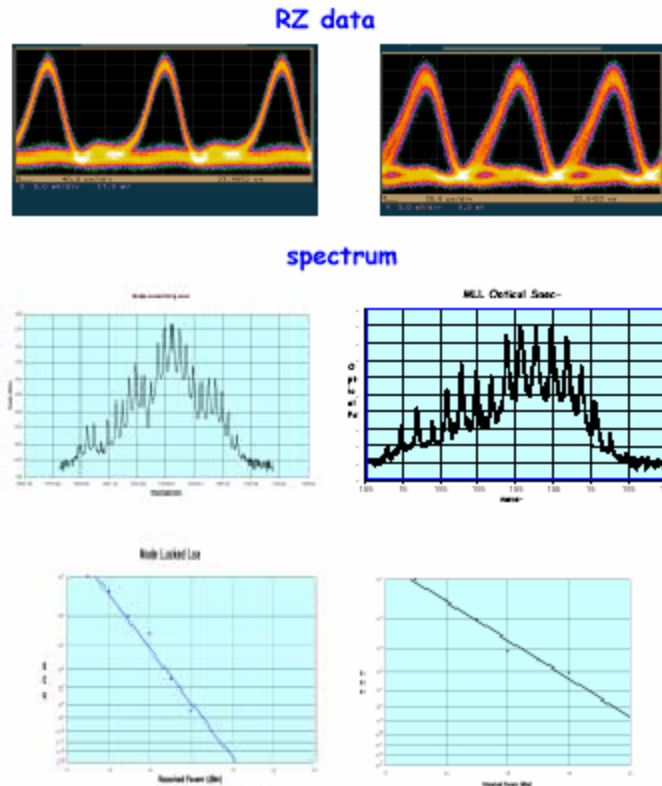


Figure 33 Recovered data, optical spectrum, and BER, using the mode locked laser of Figure 32 as a source of short pulses.

This modelocked laser can be used either as a source of many well defined and closely spaced wavelengths to be used for the wavebanding type of hierarchical multiplexing, or as a source of phase aligned frequencies for one type of OCDMA.

3.5 Assessing hierarchical multiplexing

In assessing the different approaches to hierarchical multiplexing we have considered the spectral efficiency that be obtained, the technical challenges, and the cost of additional equipment needed. We are also interested in the extent to which any or all of these multiplexing methods could coexist on a single network and coexist with “conventional” WDM. Finally, we consider the situations in which one or the other of these methods would be useful.

Ultra-high speed data: This approach, using 40 Gb/s and higher rates has the advantage that it requires only a single laser for a large amount of bandwidth. However it requires high speed modulation, which is technically challenging, and imposes tight requirements on the network performance, especially one the performnace of network elements. We have not investigated this option in detail because Professor Gary Carter is working on this.

Wavebanding: Wavebanding requires a large number of very well defined wavelengths, i.e., more lasers. Even if a single laser can be used to produce all the wavelengths, as we propose, this

approach requires multiple modulators, though at a lower modulation rate than for high-speed data, and more sophisticated multi-granularity Network Elements, capable of separating the closely spaced wavelengths. Under the DARPA-supported PEGASUS project we investigated architectures for such NE's. It is important to remember, however, that the the wavelenths in a band need not be separated at every NE; this means that the entire band can be treated as a single wavelength until it reaches the point at which its constituent wavelengths need to be retrieved. As we have demonstrated, these subchannels can travel through unmodified NE's with little or no degradation, so that usable bandwidth can be expanded with minimal cost. One requirement that wavebanding imposes on the NE's is that passbands must be as spectrally flat as possible and that polarization dependent loss must be minimized. Because of the need for additional lasers and modulators, this method seems most useful for breaking the bandwidth into modest sized subchannels. For example, breaking the 100 GHz wide MONET channels into four 25 GHz subchannels, each carrying 10 Gb/s, provides substantial increase in spectral efficiency at modest cost.

Subcarrier multiplexing: Subcarrier multiplexing allows multiple data streams to be transmitted using a single laser and modulator. However, it also requires the electronics to mix each data stream with a subcarrier and combine all into proper form to drive a modulator. The modulator, in turn, must be capable of high speeds even though the individual data streams themselves are relatively low speed, and in order to avoid mixing of the data, the modulator needs higher linearity than is normally required. One advantage of subcarrier multiplexing is that it permits transmission of any type of data format, even analog. Subcarrier multiplexing is most suitable for relatively low speed individual data streams, so that the agregate rate presented to the modulator is within the modulator bandwidth. Thus we have demonstrated it as a second order multiplexing, using one of the 25 GHz wide subchannels within our 4-subchannel division of the 100 GHz MONET channel.

OCDMA: We are only at the start of our OCDMA studies. We believe that the method we are pursuing can offer very high spectral efficiency, but it requires specialized sources and multiplexers for encoding and decoding, along with specialized detection of the decoded data. We are looking at a form of OCDMA that uses the phase relationship of the subwavelengths produced by the mode locked lasers. One advantage of this type of OCDMA is that it can coexist with conventional WDM. Since the entire coded data lies within a single WDM channel, it can pass through normal NE's along with other wavelength channels. It is clearly too early to evaluate this type of OCDMA.

3.6 Publications

We have reported on the hierarchical multiplexing work in:

Shahab Etemad, Tolga Yilmaz, Chris DePriest, and Peter Delfyett, "Mode-locked SOA as a Source for a wdm-WDM Hierarchy Architecture," OFC 2002

Paul Toliver, Robert J. Runser, Jeffrey Young, and Janet Jackel, "Experimental Field Trial of Waveband Switching and Transmission in a Transparent Reconfigurable Optical Network," submitted to OFC 2003

Shahab Etemad, Jeff Young, Tolga Yilmaz, Chris DePriest, and Peter Delfyett, Craig Price and

4 Lessons learned

The work we have done in the past two years of studying this network has led us to a deeper understanding of transparent reconfigurable networks.

Polarization: Our studies of network stability and error storms emphasized the importance of polarization in transparent networks. Even though PMD, which had anticipated might limit transmission of 10 Gb/s and over, was apparently not an issue, more subtle polarization effects, like the variation over time of the polarization arriving at any NE, and what had appeared to be manageable amounts of polarization dependent loss, interacted in the NE to make wavebanding impractical, until we moved from the polarization dependent lithium niobate switch fabrics of the Lucent NE's to the nearly polarization independent MEMS in the Firstwave NE's. Polarization dependence is likely to interfere with any spectrally efficient form of hierarchical multiplexing. Luckily, the MEMS switches, which are likely to be used in future equipment, have much better polarization performance than the Lithium Niobate switches, which are unlikely to be used.

Optical power transients: We see that optical power transients occur in many situations, including fiber cuts, network reconfiguration, bursty traffic, and in the peculiarities of certain types of data. Initially we had expected that transients would prove more of a problem when channels are dropped, but in fact we observe the opposite; the most extreme response is seen when channels are added suddenly. We also see that it is possible to control these transients through redesign of the EDFA's. The recognition of the problem of transients in transparent networks was pioneered during the earlier MONET Project. Since that time, others have recognized the problem, and some manufacturers of EDFA's are offering gain stabilized components, though none yet appear to respond quickly enough to meet our needs.

Hierarchical multiplexing: While point-to-point transmission can expand its use of bandwidth by adding wavelengths and/or increasing bit rate, transparent reconfigurable networks will need to use some form of hierarchical multiplexing in order to organize bandwidth and avoid rapidly increasing equipment costs. This is an area that needs further study; while we have investigated the transmission of hierarchically multiplexed data, we have only begun to think about the architecture of Network Elements that would be used for such networks, and others who have addressed this issue have provided only very sketchy suggestions for such NE's.

Network control and management, which was not strongly emphasized in this project, is an area that must be developed further if transparent networks are to become practical. Integrating NC&M with a more sophisticated form of optical performance monitoring is a challenge for the future.

5 Interactions with other projects

PCAD This NIST supported project grew in part from the network simulation studies started in the MONET Project. We have used the wavelength domain simulator developed within PCAD to study transient effects in the network.

PEGASUS This DARPA funded project supported our studies of wavebanding architectures for future multi-granularity network elements.

LTS The Laboratory for Telecommunications Research is one of the MONET/ATDNet nodes and the location of much of the test equipment. We have collaborated with LTS staff on much of this work, and will continue to work on the DC Network from this laboratory.

OCDMA We will shortly begin a new DARPA sponsored project on OCDMA. The ideas that led to our proposal grew from our experience with this network and our preliminary thoughts on OCDMA, motivated by Task 2.

BOSSNet A small number of our experiments involved this network. Recently we have completed a connector to BOSSNet to replace the improvised connection we have made in the past. The combination of ATDNet and BOSSNet provides a rich environment for network experiments.

6 Publications/Patents

Shahab Etemad, Tolga Yilmaz, Chris DePriest, and Peter Delfyett, “**Mode-locked SOA as a Source for a wdm-WDM Hierarchy Architecture**,” OFC 2002

Paul Toliver, Robert J. Runser, Jeffrey Young, and Janet Jackel, “Experimental Field Trial of Waveband Switching and Transmission in a Transparent Reconfigurable Optical Network,” submitted to OFC 2003

Shahab Etemad, Jeff Young, Tolga Yilmaz, Chris DePriest, and Peter Delfyett, Craig Price and Terry Turpin, “Mode-locked SOA as a Source for a wdm-WDM Hierarchy Architecture,” at NFOEC 2002

J. Jackel, T. Banwell, S. McNown, J. Perreault, “Burst Optical Packet Transport over the MONET DC Network,” ECOC 2000

J. Jackel, T. Banwell, S. McNown, J. Perreault, “All-Optical Burst Support for Optical Packets,” ECOC 2001

Patent Application: Jackel, “Saturated Amplifier Generating Burst Support Signal,” Allowed summer 2002

Mode-locked SOA as a Source for a wdm-WDM Hierarchy Architecture

Shahab Etemad

*Telcordia Technologies, Red Bank, NJ 07701
Tel: (732) 758-3262; Email: setemad@telcordia.com*

Tolga Yilmaz, Chris DePriest, and Peter Delfyett

*School of Optics/CREOL, 4000 Central Florida Blvd, Orlando, FL 32816
Tel: (407) 823-6971; Fax: (407) 823-6880; email: tolga@creol.ucf.edu*

Abstract: We describe and characterize mode-locked external cavity ring and monolithic semiconductor lasers as a multirange wavelength selectable source. The proposed source emits a tunable wave band (WDM) containing ultra-dense individually selectable micro wavelength (wdm) channels.

Mode-locked SOA as a Source for a wdm-WDM Hierarchy Architecture

Shahab Etemad

Telcordia Technologies, Red Bank, NJ 07701
Tel: (732) 758-3262; Email: setemad@telcordia.com

Tolga Yilmaz, Chris DePriest, and Peter Delfyett

School of Optics/CREOL, 4000 Central Florida Blvd, Orlando, FL 32816
Tel: (407) 823-6971; Fax: (407) 823-6880; email: tolga@creol.ucf.edu

Abstract: We describe and characterize mode-locked external cavity ring and monolithic semiconductor lasers as a multirange wavelength selectable source. The proposed source emits a tunable wave band (WDM) containing ultra-dense individually selectable micro wavelength (wdm) channels. In a wave banding architecture with N wave bands and M channels in a band such a source would replace $N \times M$ individual sources thus bringing both physical and operational savings to the network.

©2000 Optical Society of America

OCIS codes: (250.5980) Semiconductor optical amplifiers, (060.2330) Fiber optics communications

Introduction

Development of cost effective light sources with high wavelength accuracy and stability has been identified as an important step in mass deployment of reconfigurable optical networks in metropolitan area where cost of light sources and optical cross connects are still dominating factors. Recently there has been an extensive interest in traffic grouping or wave banding as a procedure to reduce the number of ports in optical cross connects wherever different traffic can share the same port. Although simulation studies of wave banding have shown promise [1], up to now every optical channel needed a light source of its own. In a network designed with M bands each containing N channels, we either need $M \times N$ fixed lasers or N tunable lasers. Whereas tunable light sources do reduce the operational cost associated with inventory and provisioning in a network, we still need to have one source per optical channel. In this paper we propose a third approach and show how mode-locked lasers can be a single source capable of emitting all of the N wavelengths within a band, which in turn can be tuned. Our proposed source is capable of generating the $N \times M$ channels of which any N channels are used at any time. In other words, such a source is capable of replacing N tunable lasers or $M \times N$ individual lasers.

Experiment

In Fig. 1a we show a mode-locked external cavity fiber ring laser that consists of a semiconductor optical amplifier (SOA) as a gain medium, an external modulator to tune the modulation rate of the gain to a resonance mode of the cavity, a WDM filter to limit the gain to a predefined spectral range and a tap to channel the output. The dotted line identifies the cavity length which is typically several meters.

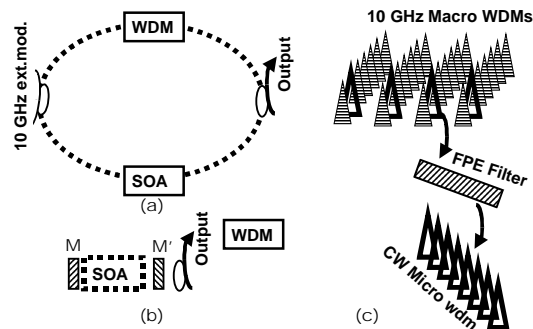


Fig. 1: (a) Mode-locked SOA ring size cavity, (b) Mode-locked SOA with chip size cavity, (c) wdm-WDM source.

Figure 2 shows the RF power spectrum of the laser mode locked with the driving frequency tuned to a cavity resonance. The two weak resonance peaks separated by ~ 8.5 MHz on either side of the locked mode are due to the longitudinal mode beating at the harmonics of the cavity frequency. From the separation between the two neighboring cavity modes one can estimate the length of the optical cavity to be about ~ 18 meters. These out of resonance cavity modes are major contributors to the high frequency noise. To suppress the out of resonance cavity modes we have considered two procedures. One is to introduce a filtering effect using a high finesse (F) Fabry Perot etalon (FPE) filter in the cavity to limit the lasing to a specific mode. This procedure is documented elsewhere [2]. The other is to reduce the effect of side modes by decreasing the cavity to the size of the SOA chip as shown in Figure 1b. This reduction in size increases the spacing between the cavity modes to frequencies comparable to that of the driving frequency, thus limiting the number of the modes to only a few. In this case the modulation of the gain is achieved through the SOA's driving current.

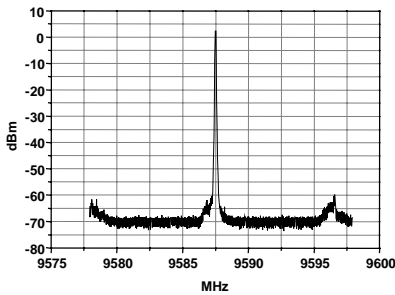


Fig. 2: RF power spectrum of the ~ 10 GHz mode-locked ring laser.

Figure 1c depicts the time and wavelength variation of the output from such lasers. In the time domain, one sees periodic transform limited pulses of light whose time resolution is limited by the spectral range of the gain medium. In the wavelength domain each pulse contains the resonance cavity modes coupled (phase locked) and separated by the driving frequency of the external modulator. The spectral content of the macro pulse can be adjusted by a macro WDM filter situated inside the cavity. The number of cavity modes that are excited affects stability of the spectral content of such a macro pulse. For example, in case of Figure 1b where because of the small size of the cavity only the fundamental mode could be present there is no contribution to the noise from harmonic modes.

The micro wavelength channel can be extracted by a well-designed FPE as shown in Figure 1c. It is the intent of this paper to characterize the time and the wavelength dependence of these so called longitudinal modes and to outline their usefulness for generating a tunable band of ultra dense but not necessarily large channel number optical networking applications.

Results and Discussion

Figure 3a shows the high-resolution optical spectrum of a mode-locked ring laser described in Figure 1a but without the WDM filter. Mode locking has been stabilized by fine tuning the driving frequency to within 1 kHz of the free spectral range (FSR ~ 11 GHz) of the FPE filter inside the cavity. To our knowledge this is the first report of a mode-locked SOA ring laser where the extraneous cavity modes have successfully been suppressed. The 18 micro wavelengths shown in the 1.5 nm range are part of a total of about 40 modes defining the macro pulse. Note that by limiting the gain spectrum and decreasing the number of micro wavelengths one can increase their intensity.

Figure 3b shows the high-resolution optical spectrum of a mode-locked "chip" laser described in Figure 1b. Here, the mirror coating of the back facet and the 90% reflecting output coupler in front of the chip define the cavity. In this case the cavity modes are separated by 1.3 GHz and harmonic mode locking is achieved at 9.2 GHz by modulating the SOA's driving current. The 39 micro wavelengths in the 3 nm range are part of a macro pulse with duration of ~ 10 ps as measured by an autocorrelator. Comparing the two methods of generating micro wavelengths we find the "chip" laser to be more stable than the ring laser at this time

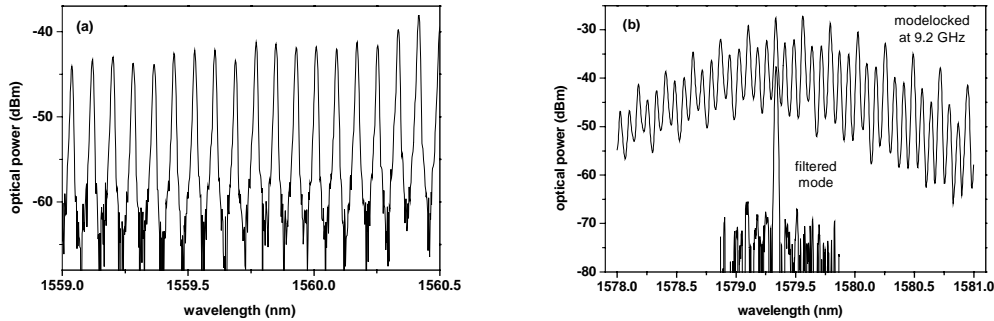


Fig. 3: (a) The optical spectrum of the 10 GHz mode-locked ring laser with an intracavity FPE; (b) optical spectrum of the mode-locked “chip” laser with the full spectrum showing many wdm micro wavelengths and FPE filtered spectrum showing a single micro wavelength.

In Figure 3b we also show a single micro wavelength selected by cascading two FPEs, one with FSR=200 GHz and F=40 and the other FSR=11 GHz and F=181 that we had available. Note that similar extraction can be obtained using a single FPE and a notch filter. The optically amplified single micro wavelength has a signal to noise ratio of better than 30 dB and is a continuous wave by its nature. It is the superposition of all these phase locked CW micro wavelengths (wdm) that constitutes a macro pulse (WDM) with its power spectrum at the driving frequency as shown in Figure 2. We find no signal at the 9.2 GHz driving frequency or its harmonic associated with macro pulse. Any RF component of the micro wavelength is less than 30 dB of the macro pulse.

We propose to use such micro wavelengths as carriers for high bit rate transmission in a wdm-WDM hierarchy architecture. In such architecture at the egress a band of micro wavelengths are generated by a single source. Individual micro wavelengths are separated and modulated using external modulators then recombined and routed together through the network. That all micro wavelengths are generated by the same gain medium has the advantage of not being affected by polarization drift associated with wave banding schemes using individual sources. From an operational point of view we note that the inventory and provisioning issues are much easier to handle since it is the same single source that is used at every node.

A recent transmission experiment using a 25 GHz spaced micro wavelengths extracted from a super continuum, emphasized the large number of available channels [3]. In contrast in our proposal we emphasize the wave banding possibility that a device shown in Figure 1c can offer. Wave banding architectures offer cost saving scenarios where a number of micro channels share the same ride through the same port of an optical cross connect [1]. By using the macro filter WDM one can select a band of micro wavelengths anywhere in the gain spectrum of the SOA. Note that the number of micro wavelengths within a band is only limited by the choice of intracavity FPE filter and the required band pass for a given bit rate associated with the data. In this study we have used a tunable FPE suitable for ten OC-48 channels within the 1 nm band pass of our experimental network. Other applications requiring transmission of many more channels at lower bit rate through the same 1 nm band pass is possible with this novel source.

References

- [1] L. Noirie, M. Vigoureux, E. Dotaro, “Impact of intermediate traffic grouping on the dimensioning of multi-granularity optical networks”, OFC TuG3-1 (2001).
- [2] G. T. Harvey, Linn F. Mollenauer, “Harmonically mode-locked fiber ring laser with an internal Fabry-Perot stabilizer for soliton transmission”, Opt. Lett. **18**, 107 (1993).
- [3] H. Takara, E. Yamada, T. Ohara, K. Sato, K. Jinguji, Y. Inoue, T. Shibata, and T. Morioka, “106x10 Gbit/s, 25 GHz-spaced, 640 km DWDM transmission employing a single supercontinuum multi-carrier source”, CLEO CPD11-1 (2001).

Experimental Field Trial of Waveband Switching and Transmission in a Transparent Reconfigurable Optical Network

Paul Toliver, Robert J. Runser, Jeffrey Young, and Janet Jackel

Telcordia Technologies, 331 Newman Springs Rd., Red Bank, NJ 07701

Tel: (732) 758-3057; Fax: (732) 758-4372; email: ptoliver@research.telcordia.com

Abstract: We demonstrate 4-channel, 25GHz-spaced waveband transmission in a 200GHz passband through a transparent reconfigurable optical network. We investigate the impact of polarization effects on the waveband and its interaction with MEMS and LiNbO₃ switch fabrics.

Introduction

Waveband switching is a technique in which a subset of wavelengths are grouped together and switched optically as a single entity through a transparent network infrastructure. The individual wavelengths of a waveband are commonly assumed to be contiguous in spectrum, although they could also be interleaved or arbitrarily spaced. One of the key advantages of switching groups of wavelengths that share a common multi-hop path rather than individual wavelengths is that fewer ports are required on the switch fabrics of photonic cross-connects at transit nodes. Wavebands can also be used to upgrade the capacity of existing transparent networks without requiring any changes to the core network elements provided the waveband signals generated at the edge fit within the allowable optical passbands. This technique can also be used to support higher channel bandwidths on fiber paths that would otherwise require costly impairment compensation or regeneration.

The benefits of waveband switching have been studied by a number of groups from an architectural perspective [1, 2]. To date, however, there have been few reports discussing the practical implementation issues over real networks. Here, we present the results of waveband switching experiments that were demonstrated on the Advanced Technology Demonstration Network (ATDnet)—an optical network testbed that links a number of government agency laboratories in the Washington, D.C. metropolitan area (see Fig. 1). Under the MONET program, the original ATDnet testbed was designed to support only 8 x 2.5 Gb/s wavelengths per fiber [3]. The infrastructure of the East Ring supports network elements (NEs) that are optically transparent enabling the possibility for considerably higher bandwidths but with the need for external dispersion compensating elements. For the particular results summarized in this paper, the waveband switching experiments primarily utilized paths through the MEMS and LiNbO₃-based transparent wavelength selective cross-connects (WSXC) located at both the Laboratory for Telecommunication Sciences (LTS) and the Naval Research Laboratory (NRL).

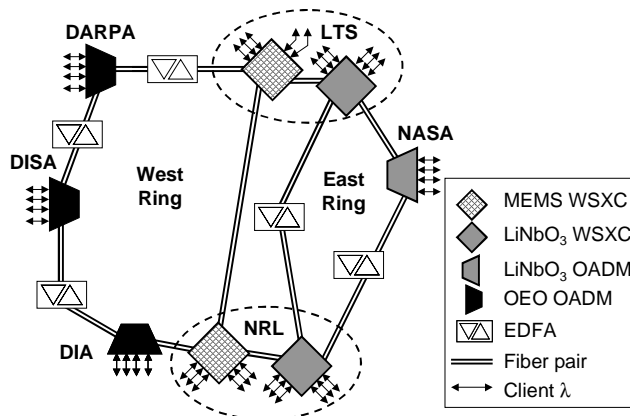


Fig. 1. ATDnet testbed comprised of both transparent and non-transparent network elements.

Experiment

The transparent network elements within ATDnet are capable of supporting at least 8 wavelength passbands on a 200 GHz ITU frequency grid. We performed our waveband switching experiments using the second 200 GHz window, which is centered at 1550.92 nm, while other single wavelength signals, such as OC-48 ATM, populated the remaining seven spectral windows.

As illustrated in Fig. 2, a 4-channel waveband transmitter (WB Tx) and a 4-channel waveband receiver (WB Rx) were constructed and connected to the add/drop ports of a WSXC

located at the LTS. The WSXC allowed us to switch the waveband signal through various transparent paths of ATDnet. The four sub-channels of the WB Tx, which consists of an array of tunable lasers followed by an array of electro-optic modulators, are passively multiplexed together on a 25 GHz grid and their amplitudes are equalized before the WSXC add port. The WB Rx consists of a cascaded array of fiber Bragg grating filters (each 15 GHz wide) and circulators along with an array of four photoreceivers. Since the ATDnet NEs are optically transparent, no changes or hardware upgrades were required to support the waveband client signal. Such an upgrade would have been impossible given an OEO switched network.

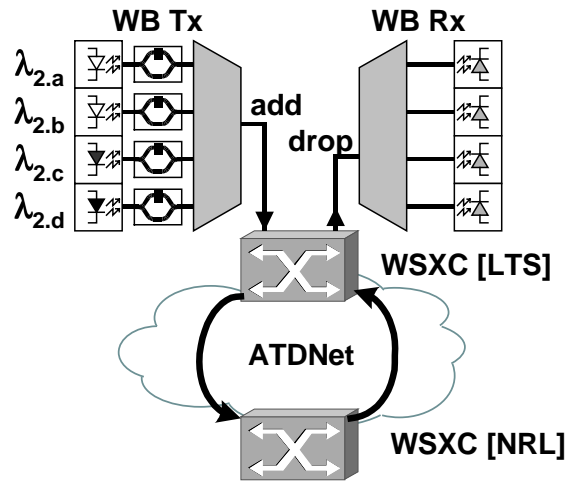


Fig. 2. Experimental setup for waveband switching demonstration.

Results

In Figure 3, we show the 4-channel waveband signal contained within a spectral window that is approximately 120 GHz wide and centered at 1550.92 nm. This particular window is defined by the optical mux and demux components inside the MEMS-based WSXC. As shown by the “add” signal plot, the four waveband sub-channels are set to the following wavelengths: $\lambda_{2a}=1550.52$, $\lambda_{2b}=1550.72$, $\lambda_{2c}=1550.92$, and $\lambda_{2d}=1551.12$ nm. The waveband was transmitted over approximately 100 km of SMF-28 fiber on a loopback path between the LTS and NRL through MEMS-based WSXCs located at each node. The entire waveband is received at the drop port, although the λ_{2a} sub-channel is attenuated slightly due to its proximity to the passband edge of the NE muxes and demuxes.

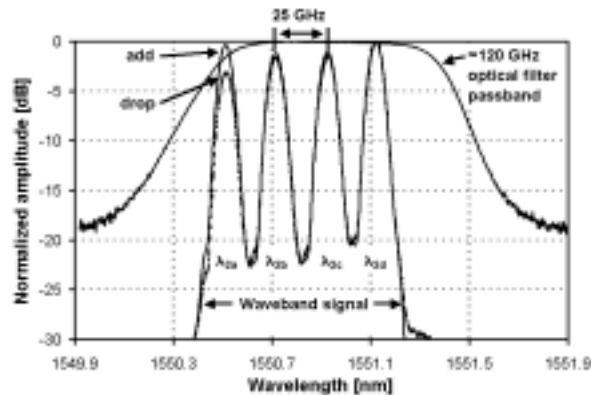


Fig. 3. Plot of add/drop waveband spectrums and passband spectral window.

The recovered bit error rates (BERs) of all four sub-channels after transmission through the two WSXCs, 100 km of fiber, and optical amplifiers (integrated into the NEs) is shown in Fig. 4. For these BER results, the waveband sub-channels are modulated with decorrelated OC-48 (2.488 Gb/s) pseudo-random data streams ($2^{23}-1$). The average receiver sensitivity given a BER of 10^9 is -34.4 dBm. Compared to back-to-back operation, the power penalty for the four sub-channels is only 0.1 dB. This experiment demonstrates that an existing transparent network infrastructure originally designed for 2.5 Gb/s capacity per passband can support 10 Gb/s per passband using wavebanding techniques at the edge of the network without requiring changes to core network elements or transmission fibers.

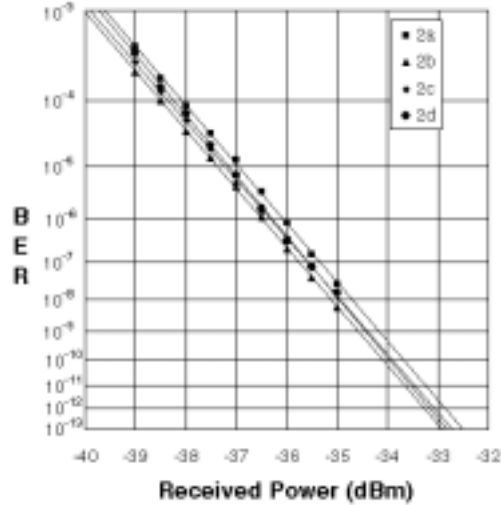


Fig. 4. Bit error rate performance with four 2.5 Gb/s channels in waveband.

We also investigated the ability to modulate the individual sub-channels at 10 Gb/s, which provides a total passband capacity of 40 Gb/s within the transmission window. In this experiment, all four wavelengths were modulated by through a common 10 Gb/s electro-optic modulator. Pre- and post-dispersion compensating fibers were used to support the 10 Gb/s sub-channels over the 100 km SMF-28 network span. The resulting BER performance for the four 10 Gb/s sub-channels is summarized in Fig. 5. The average receiver sensitivity at a BER of $10E-9$ is -17.8 dBm. The average power penalty across the four sub-channels was 1.1 dB, with λ_{2a} having the largest penalty of 1.5 dB. The increased power penalty is likely to be a result of the channel proximity to the passband edge causing greater signal distortion due to filter dispersion. It would not have been possible to achieve the transmission of a single 40 Gb/s wavelength within an ATDnet passband without subsequent compensation for PMD.

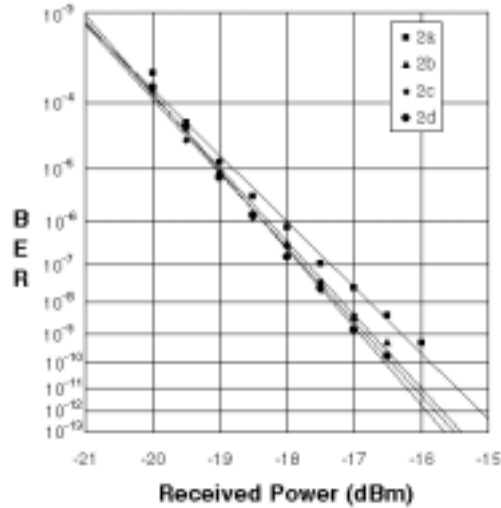


Fig. 5. Bit error rate performance of four 10 Gb/s sub-channels of the waveband.

Impact of polarization effects

An important physical layer issue to consider in a waveband switched network is the impact of how impairments may impact individual sub-channels of the waveband differently. In particular, polarization effects such as polarization dependent loss (PDL) can be particularly important for transparent NEs that use optical switch fabrics such as LiNbO₃. The ATDnet contains NEs with both MEMS and LiNbO₃ fabric technologies. The PDL for the loopback path for the MEMS-based WSXCs was less than 0.5 dB for waveband sub-channels λ_{2b} , λ_{2c} , and λ_{2d} and did not vary significantly based on the launched polarization orientation of the subchannels. The first sub-channel (λ_{2a}) had a higher PDL value of 1.0 dB due to its proximity to the passband edge. In contrast, when the signal was sent through the LiNbO₃-based WSXC, the PDL varied within the range of 4.0-5.5 dB across the waveband. The amount of PDL experienced by each sub-channel was a function of the launch polarization orientation.

Ensuring that the sub-channels of a waveband maintain the same amplitude is important for minimizing the waveband transmission penalty. Over longer spans and multiple hops through optical networks, the amount of PDL through a network element should be kept to a minimum especially since it can coupled with second order PMD (which introduces wavelength dependent depolarization [4]) to cause additional variation in the sub-channel amplitudes.

Conclusion

Wavebanding is a technique that can be applied to existing transparent optical elements to increase the spectral efficiency within a passband without requiring costly impairment compensation or upgrades to photonic cross-connects. It can also be applied to new network designs in order to minimize the number of switch fabric ports. We have demonstrated 4-channel waveband transmission over 100 km of legacy fiber in ATDnet within a 200 GHz optical passband with aggregate capacities of 10 and 40 Gb/s. Understanding the impact of impairments and optical nonlinearities that may affect the individual sub-channels of a waveband is important for determining the ultimate reach, capacity, and channel spacing that can be achieved within a passband of existing networks and fiber infrastructure.

This work has been supported in part by the LTS and also by DARPA under contract F30602-00-C-0167. The authors gratefully acknowledge Matthew Goodman of Telcordia Technologies and Scott McNown of the LTS for valuable technical discussions and support.

References

- [1] L. Noirie, M. Vigoureux, and E. Dotaro, *OFC 2001*, paper TuG3, March 2001.
- [2] R. Lingampalli and P. Vengalam, *OFC 2002*, paper ThP4, March 2002.
- [3] W. T. Andersen, J. Jackel, G.-K. Chang, et al., *J. Lightwav. Technol.*, vol. 18, no. 12, pp. 1988-2009, Dec. 2000.
- [4] C. D. Poole, N. S. Bergano, R. E. Wagner, and H. J. Schulte, *J. Lightwav. Technol.*, vol. 6, no. 7, pp. 1185-1190, July 1988.

BURST OPTICAL PACKET TRANSPORT OVER THE MONET DC NETWORK

J. Jackel, T. Banwell, Telcordia Technologies, Inc., Red Bank, NJ, USA

S. McNowan, National Security Agency, Ft. Meade, MD, USA

J. Perrault, Laboratory for Telecommunications Research, Adelphi, MD, USA

Abstract

We demonstrate here an optical burst support technique that allows error free transmission of bursty traffic on routes within the MONET/ATDNet DC Network which are otherwise incapable of supporting such traffic

Optical networks are often intolerant of bursty optical signals and may exhibit rapid time-dependent gain variations which impair transmission of burst optical packets. The MONET WDM testbed has several routes which exhibit this limitation. In this paper, we demonstrate "Optical Burst Support" using a closely spaced WDM optical signal substitution within the same wavelength channel to eliminate burst induced gain variation. Error free transmission of 21 kb optical packets at 700 Mb/s are demonstrated over susceptible MONET routes.

The MONET/ATDNet DC Network is an eight wavelength, rapidly reconfigurable, WDM network designed for rate and protocol transparent optical communication. There is substantial interest in extending the utility of this network beyond traditional optical streams to optical burst packet transport and perhaps optical packet switching. However, both experiments and simulations have shown that on certain routes within this network bursty input power leads to degradation on both the bursty data and of data on other channels traversing the same route.^{1 2} Degradation of this kind has also previously been discussed for packetized traffic traversing many EDFAs.³

Within the MONET/ATDNet DC Network two methods are used to stabilize EDFA gain in WDM network elements: all-optical gain clamping, with a response time of tens of μs , and a slower (1-5 ms) pump-power regulation. There are compromises between in available gain, gain stability, noise figure, dynamic range and response time with each approach. Rapid changes in input optical power can disturb amplifier gain resulting in unwanted modulation of the bursty signal as well as other signals simultaneously traversing the amplifier.

Fig. 1(a) illustrates this instability. The 240 μs optical burst is sent through a 3-node MONET route optimized for continuous optical streams. Gain peaking followed by depletion and gain oscillations are apparent. Even with a fast tracking receiver, substantial bit-

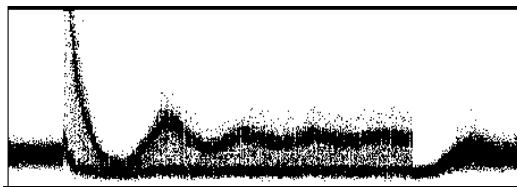


Figure 1 240 μs data burst after traversing three MONET nodes; 300 μs total time. Input is same as Fig. 3(a).

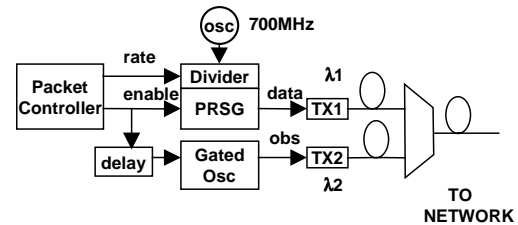


Figure 2 Burst support transmitter

errors arise during the amplitude transient. Other wavelengths traversing the same route are affected in a similar way, although less severely.

This instability occurs because power changes within a single wavelength channel affect the gain both for that wavelength and for other wavelengths through cross gain saturation in common EDFAs within and between the nodes. We show here that "optical burst support" using a second independent but closely spaced WDM optical ballast signal which compliments the burst signal's average power allows bursts to pass unerrored through this network.

The circuit in Fig. 2 creates optical burst packets and a burst support signal for maintaining constant average optical power. The circuit includes a 700MHz clock, programmable frequency divider, gated maximal length pseudo-random sequence (ML-PRS) generator and transmitter for creating variable rate and variable length packets at $\lambda_1 = 1557.0 \text{ nm}$. Packet size is con-

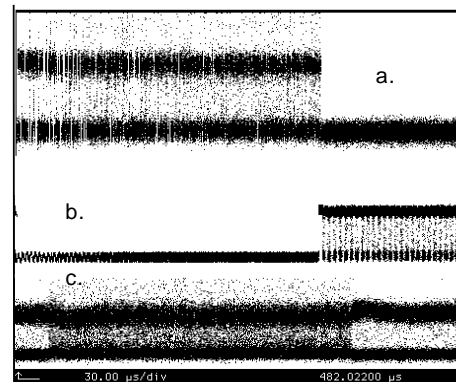


Figure 3 (a) input data burst; (b) burst support signal; returned optical signal after traversing same path as for Fig. 1.

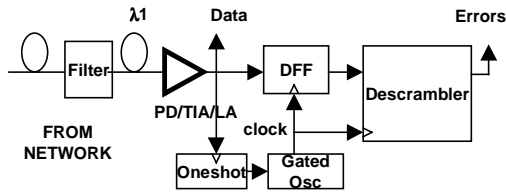


Figure 4 Burst receiver

trolled by an enable signal which also disables a 20 MHz oscillator that drives a second transmitter operating at $\lambda_2 = \lambda_1 + 0.5\text{nm}$. The oscillator disable has a programmable delay, allowing a wide range of network responses to be emulated. At 0.5 nm separation, both signals fall within the MONET passband and consequently both pass through the same path on the network and experience approximately the same losses. A 240 μsec optical burst and corresponding burst support signal are shown in Figs. 3(a) and (b), respectively, prior to optical combining. Fig. 3(c) shows the resulting network response to the composite signal; induced amplitude transients are suppressed. Fig. 4 illustrates the custom burst receiver⁴ used for measuring bit-errors in the received optical packet. It includes a wavelength filter, detector, wideband TIA and limiting amplifier with 1-100 μs threshold tracking, a clock recovery circuit consisting of a 700 ps oneshot and 700/350/233 MHz gated oscillator, and a descrambler serving as a ML-PRS decoder. The descrambler output is low for an unerrored maximal length PRS input and produces three high bits for each input bit-error.

Fig. 5 illustrates the typical behavior for a 240 μs packet at 700 Mb/s (21kBytes) received over any MONET route. The filtered optical signal in 6(a) is free of amplitude modulation. Fig. 6(b) shows the electrical signal from the limiting amplifier while 6(c) is the corresponding descrambler output. While deviation from a ML-PRS is evident preceding and following the packet, the descrambler rapidly synchronizes to the packet and no errors are detected within the packet. Power penalty curves are shown in Fig. 6 for worse case routes with slow pump power gain control (curve A), gain clamped amplifiers (B), and corresponding

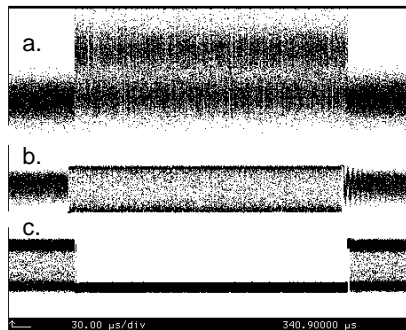


Figure 5 240 μs burst supported packet received after traversing the same path as for Figures 1 and 3(c). (a) Filtered optical signal; (b) electrical signal after limiting amplifier; (c) descrambler output showing error free operation.

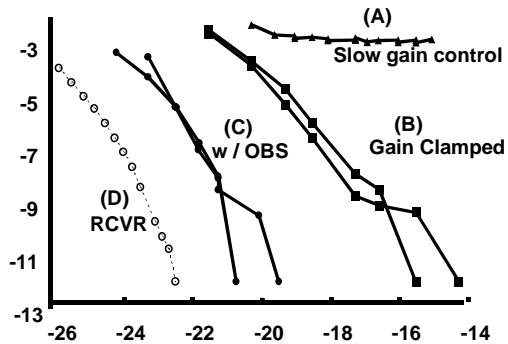


Figure 6 BER curves for (A) signal traversing path of Figures 1 and 3(c), with only slow gain control; (B) results for a similar path with gain clamped EDFAs; (C) with optical burst support and (D) back to back.

routes with optical burst support (C) and for the receiver by itself (D). Intrinsic receiver sensitivity is -23.5 dBm. Curve (A) shows that without burst support, packets sent over some MONET routes with course load balancing experience a 10^{-2} error floor. Routes containing only gain clamped amplifiers may experience a 6.5 dB power penalty, as seen in curves (B), which show performance under slightly different conditions. As shown by the two curves (C), OBS decreases the power penalty to 2.5 dB in either case. Gated oscillators have poor jitter rejection which may account for some of the 2.5 dB penalty.

Discussion

EDFA containing WDM networks designed for transparent transmission of optical streams may impose limitations on transport of bursty optical packets. While EDFAs are immune to the bit-level interference experienced by SOAs in multiwavelength operation, they are susceptible to gain variations when there are variations in optical input power, time-integrated over many bits. We have demonstrated that optical burst support in which the integrated optical power is held constant using a complementary optical signal at a wavelength in the same wavelength channel can alleviate this problem on MONET routes. This substitution need not be accurate on at bit level, as is needed in SOAs⁵ and is therefore simpler to implement. Use of optical burst support will allow us to implement a burst optical packet sub-network within the MONET/ATDNet infrastructure.

¹W. T. Anderson, et. al., "The MONET Project--A Final Report," IEEE J. Lightwave Technol., to be published.

²D. H. Richards, et. al., in Optical Amplifiers and Their Applications, Quebec, paper JWA3, pp. 206-208, 2000.

³L. Tancevski, A. Bononi, L. A. Rusch, ECOC'98, Madrid, pp. 553-554

⁴T. C. Banwell and N. K. Cheung, IEEE Photon. Technol. Lett., vol. 11, no. 11, pp. 1500-1502, 1999.

⁵H. Kim and S. Chandrasekhar in Optical Amplifiers and Their Applications, Quebec, paper OTuB3, pp. 120-122, 2000.

All-Optical Burst Support for Optical Packets

J. L. Jackel (1), T. C. Banwell(2), S. R. McNown (3), J. A. Perreault (4)

(1) Telcordia Technologies, Inc, Red Bank, NJ, USA (jackel@research.telcordia.com)

(2) Telcordia Technologies, Inc. (bct@)research.telcordia.com)

(3,4) US Dept. of Defense (srmcnow@alpha.ncsc.mil,jap@afterlife.ncsc.mil)

Abstract: We demonstrate error free transmission of multirate optical bursts over a metropolitan WDM network with EDFAs designed for constant average power by using an all-optical means for optical signal stabilization.

Growing interest in packet/burst transmission on multiwavelength optical networks has stimulated questions about the ability of optical networks to carry such bursts without degradation and without their causing degradation of data carried on other wavelengths. Optical networks containing EDFAs are typically intolerant of bursty optical signals. Rapid time-dependent gain variations in the presence of optical power variations impair transmission both of burst optical packets and of data carried on co-propagating channels./1/ Recently we demonstrated an opto-electronic method of "Optical Burst Support" using a closely spaced WDM optical signal substitution within the same wavelength channel to eliminate burst induced gain variation./2/ However, this implementation relied on data-link layer access to coordinate substitution and may not be applicable to a majority of network interfaces.

In this paper we demonstrate an all-optical form of burst support, using a saturated SOA both to amplify the input bursts and to generate a burst support signal in the absence of input optical power. This form of burst support can be used with any line rate or format and does not require access to the data-link layer. All-optical burst support has been used along with a rate agile transmitter and receiver to test the limits of optical burst transmission in this network. Error free transmission of optical packets at 233-700 Mb/s are demonstrated over susceptible routes on the MONET/ATDNet DC Network.

Fig. 1a shows how optical burst support (OBS) can be provided optically, using an SOA in an optical feedback loop to produce an optical support signal at a wavelength which shares an optical channel with the data. Unlike a fixed gain SOA, which can be made with the same structure, the OBS-SOA has the SOA gain and feedback loop loss balanced such that there is no lasing when an input signal is present at the expected power level. When the input signal is absent, the OBS-SOA lases, producing a power replacement for the signal. The OBS replacement wavelength is offset from the data signal but lies within the same wavelength channel as the data, so that it replaces prolonged gaps in the data over the entire path the data takes. Thus, any EDFA on the path sees constant input power in the channel whether the burst is present or absent, and gain fluctuations are prevented. Fig. 1b shows the output of the OBS after passing through two EDFAs for a 6.4 μ s burst. Substitution is accurate and rapid. Time for substitution to occur is less than one μ s, much less than the time for EDFA gain to respond to a loss of power. The wavelength offset prevents data signal degradation due to multipath interference from the feedback loop.

Fig. 2 shows optical bursts of 240 μ s duration, and the errors associated with them, after the bursts have traveled from NSA to NASA (two of the MONET/ATDNet nodes

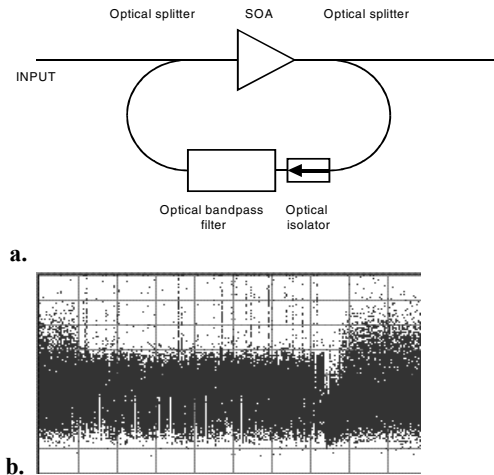


Figure 1: (a) Structure of the SOA-OBS, (b) output of SOA-OBS after passing through 2 EDFAs.

and back, with and without OBS. The bursts pass through six EDFAs on this path; two single channel saturated EDFAs as the signals are added to and dropped from the NSA node, 2 multichannel EDFAs at the ingress and egress interfaces at NSA facing NASA, and 2 multichannel EDFAs at the NASA interfaces facing NSA. Although this is a relatively short path, gain peaking followed by depletion and gain oscillations are apparent in the absence of OBS (Fig. 2a) but are almost completely eliminated with OBS (Fig. 2c). Both figures show the total optical power received within the wavelength channel. Without optical burst support there is optical power outside the burst (first 200 and final 100 μ s) because of the build up of EDFA ASE over the path. However, gain variations induced in the first EDFA are preserved and magnified over the path, and the burst show large power variations during its first 50 μ s. Where OBS is used

(Fig. 2c), the power substitution is provided before the first EDFA, and the nearly time-constant power over the entire path minimizes gain fluctuation. The minor output power variations during the first part of the burst result from imperfect substitution and/or slightly different gain/loss for the signal and OBS over the optical path. Indeed, we have verified that polarization dependent loss within network elements can subvert OBS, when the polarizations of signal and substitute wavelengths are different at the network input or drift away from each other after propagating through many kilometers of fiber.

Figures 2b and 2d compare errors for the two cases. Without OBS (Fig. 2b) there are large numbers of errors about 30-40 μ s after the start of the burst; this corresponds to the time when the optical power has been driven low.

Even with the fast tracking receiver, substantial bit-errors arise during the amplitude transient. In comparison, errors

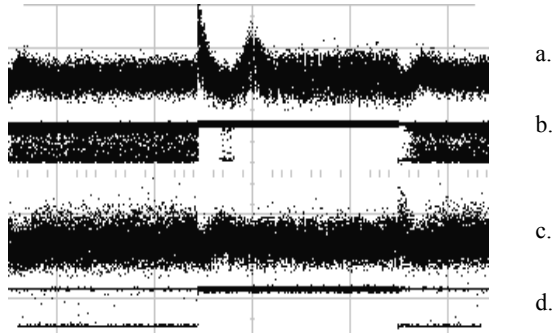


Fig 2. Optical burst after NSA-NASA-NSA round trip. (a) Returned burst without SOA-OBS, (b) associated errors (low level indicates errored bits), (c) returned burst with SOA-OBS, and (d) indication that error free transmission is occurring (high level during burst).

are absent during the burst when SOA-OBS is used (Fig. 2d), except a small number, which cannot be seen on this time scale, at the beginning of the burst when the receiver has not yet recovered the clock. While the burst itself is error free, the periods with no data, preceding and following the burst, are of course completely randomly errored.

On multi-wavelength paths through the network, other wavelengths traversing the same route are also degraded, although less severely, in the absence of burst support, because they share burst-induced time varying gain in common EDFAs. Figure 3 compares the errors on a second wavelength path in the presence of an optical burst, with and without SOA-OBS. The received power has been set so that small numbers of errors are recorded. When SOA-OBS is used, errors are uniform over the whole time (Fig. 3d), indicating that the burst creates no additional errors; without SOA-OBS there are additional errors during the burst (Fig. 3b), with the greatest number at the beginning of the burst. Fig. 3a and 3c show the corresponding errors on the burst itself, without (3a) and with (3c) SOA-OBS; the time alignment of the burst and the errors on the accompanying data without burst support is evident. Fig. 3e shows time resolved BER measurements made on the accompanying channel, with and without SOA-OBS, during two periods: "A" in the first third of the burst, where errors are densest, and "B" in the second two thirds. In the absence of burst support, errors in the accompanying channel are increased in the period immediately after the start of a burst and there is a hint of an error floor. Later in the burst the accompanying channel experiences a lower error rate, but there is still an increase relative to the error rate without a burst. With burst support, errors are much lower and are the same, within measurement accuracy, during both A and B; errors with SOA-OBS are identical to those without any bursts present (not shown) indicating that the SOA-OBS is successful in replacing the optical power in the channel

While WDM networks containing EDFAs may impose limitations on transport of bursty optical packets, we show that use of a semiconductor optical amplifier to provide all-optical burst support can eliminate degradations both to the burst data and to data in other channels sharing the same EDFAs. This SOA-OBS need be provided only at the input to the network, since the presence of a complementary optical signal at a wavelength within the same wavelength channel maintains a constant input power to all the EDFAs

in the burst's path, so long as excess filter passband induced or polarization dependent loss does not destroy the optical power balance. A subchannel optical filter must also be employed at the output of the network in order to remove the power balancing wavelength. SOA-OBS can provide burst support at essentially any rate and for bursts of any duration and spacing; it enables an even wider range of transparency than previous opto-electronic burst support. SOA-OBS thus makes it possible for transparent optical networks initially designed only for provisioned wavelengths to transport optical power bursts without degradation.

Acknowledgements: This work was supported in part by DARPA under contract F30602-99-C-0167, and by LTS contract MDA904-99-C-2582. We thank M. Lukacs for technical

references

- /1/ W. T. Anderson, et. al., "The MONET Project – A Final Report," J. Lightwave Technol., vol. 18, pp. 1988-2009, 2000.
- /2/ J. Jackel, T. Banwell, S. McNowen, J. Perreault, "Burst Optical Packet Transmission over the MONET DC Network," ECOC2000, Munich, Postdeadline paper 29

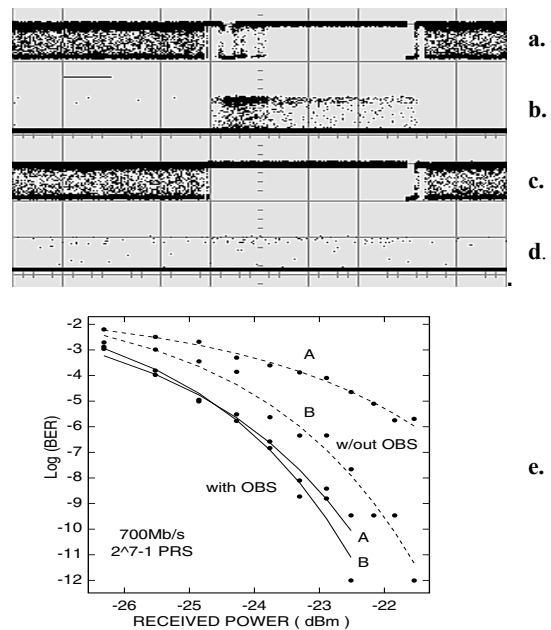


Fig. 3 Error detection for (a) burst and (b) accompanying channel without burst support on burst channel, (c) burst and (d) accompanying channel, with SOA-OBS on the burst. (e) Time resolved BER measurements for (b) and (d) taken using histograms for intervals A and B.